Modelling Snow Water Conservation on the Canadian Prairies

Centre for Hydrology Report No. 11

John Pomeroy, Xing Fang, and Brad Williams

Centre for Hydrology
University of Saskatchewan
117 Science Place
Saskatoon, SK
S7N 5C8

April 29, 2011

Modelling Snow Water Conservation on the Canadian Prairies

Centre for Hydrology Report No. 11

Prepared for

John Kort and Gary Bank
Agriculture and Agri-Food Canada

Prepared by

John Pomeroy, Xing Fang, and Brad Williams

University of Saskatchewan
Saskatoon, Saskatchewan
April 29, 2011

1 Introduction

Snowcover accumulation has tremendous impacts on Canadian Prairie hydrology and agriculture (Pomeroy and Gray, 1995; Fang and Pomeroy, 2007). Wind redistribution of snow or blowing snow is frequent in the Prairies and controls the accumulation of snowcover. Blowing snow transport is normally accompanied by in-transit sublimation (Dyunin, 1959; Schmidt, 1972; Pomeroy, 1989). Blowing snow transport and sublimation result in losses to exposed snowcovers from erosion of from 30% to 75% of annual snowfall in prairie and steppe environments (Tabler, 1975; Pomeroy et al., 1993). The disposition of this eroded snow to either sublimation or transport and subsequent deposition is important to surface water budgets. Transported snow is available for snowmelt, while that sublimated is returned to the atmosphere. Blowing snow fetch, or the downwind distance of uniform terrain that permits snow transport, determines the disposition between sublimation and transport, longer fetches promoting greater sublimation per unit area (Tabler, 1975; Pomeroy and Gray, 1995).

Calculation of blowing snow fluxes (erosion, transport, sublimation) for a uniform area, using the presumption of horizontal steady state flow (Pomeroy, 1989), does not provide sufficient information to calculate the snow cover mass balance over larger areas where flow at many points in the landscape will deviate significantly from steady state conditions. Schemes have been developed to calculate blowing snow fluxes over terrain of varying fetch and land use (Pomeroy et al., 1993) and varying terrain (Liston and Sturm, 1998; Essery et al., 1999; Fang and Pomeroy, 2009). For example, the computationally intensive schemes presented by Pomeroy et al. (1993), Liston and Sturm (1998), Essery et al. (1999) and Fang and Pomeroy (2009) calculate fluxes using physically-based algorithms for a series of downwind control volumes; the downwind boundary condition at one control volume is the upwind boundary condition of the next. A drawback of these schemes is that some of the input parameters (threshold wind speed for transport, occurrence of blowing snow] are not normally available from meteorological records. Li and Pomeroy (1997a) present a method to directly calculate threshold conditions for snow transport from the meteorological history of snowpacks, while Li and Pomeroy (1997b) calculate the probability of blowing snow occurrence using similar data. A comprehensive model of blowing snow was assembled by Pomeroy and Li (2000) and tested extensively in the Prairie and Arctic environments where it was shown to accurately predict snow accumulation. Subsequent tests by Fang and Pomeroy (2009) show that the model can accurately predict snow accumulation in a wide range of prairie to partly wooded environments.

Adaptation of these methods permits the application of physically based blowing snow algorithms driven by standard meteorological data sets and provides a method for scaling blowing snow fluxes from a point to larger areas including sites with various shelterbelt spacings. This project compares field measurements of snow distribution, associated with shelterbelts at various spacings, to modeled results of snow redistribution by wind. Virtual shelterbelt configurations modeled with real climate data examine the likely impacts of shelterbelt systems on snow water conservation over multi-year time periods including drought and snowy years.

2 Study Site and Data

2.1 Study Site

The study was conducted on cultivated fields near Conquest, Saskatchewan (51˚31.8'N, 107˚14.9'W, 570 m a.s.l), which is approximately 11 km west of the Town of Outlook and 51 km east of the Town of Rosetown (Figure 1). Two continuously cropped agricultural sites, one with widely spaced shelterbelts and one with narrowly spaced shelterbelts, were chosen. The widely spaced shelterbelt site consists of two fields with a single shelterbelt between them, while the narrowly spaced shelterbelt site has four shelterbelts at various spacings and four fields in-between the shelterbelts (Figure 2). In the fall of 2010 at the widely spaced shelterbelt site, the cropped fields (open fields 1 and 2) were covered with 0.01-m tall stubble and the single shelterbelt was a 5-m tall dense Caragana hedge. At the narrowly spaced shelterbelt site, fields 1 and 2 were covered with 0.01-m tall lentil stubble and open fields 3 and 4 with 0.3 m to 0.2-m tall wheat stubble. Shelterbelt 2 was a 4.5 m tall Caragana hedge, and shelterbelts 3 and 4 were a mix of 20-m tall elm trees with 10-m tall Caragana hedge. All shelterbelts had a horizontal porosity between 30 to 40%.

Figure 1. Location of study site: Conquest, Saskatchewan.

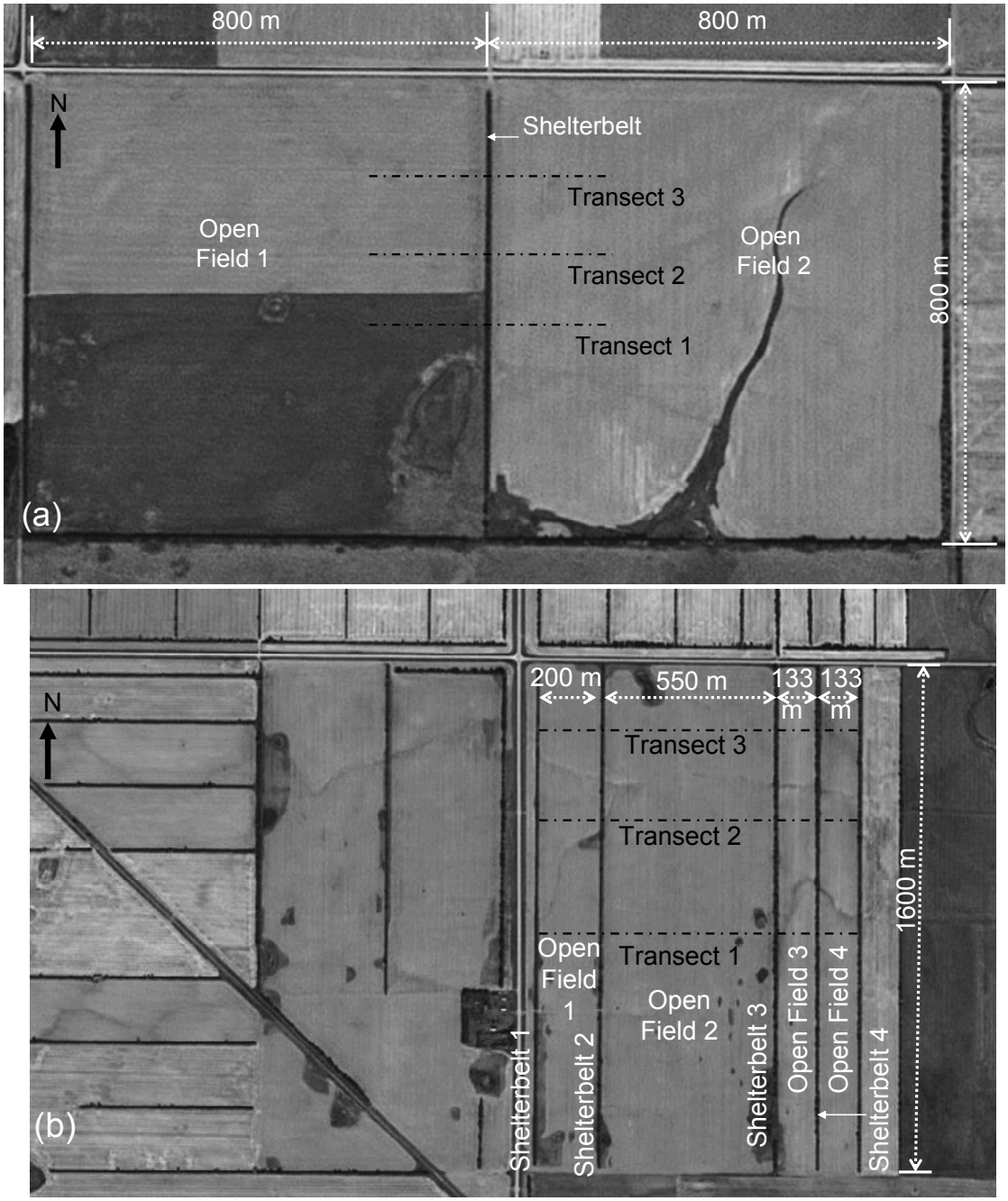

Figure 2. Shelterbelt sites at Conquest, Saskatchewan: (a) widely spaced shelterbelt site and (b) narrowly spaced shelterbelt site.

2.2. Meteorological and Field Observation Data

2.2.1 Meteorological Data

Meteorological data collected at Outlook PFRA and Rosetown East stations were downloaded from the 'National Climate Data and Information Archive' (www.climate.weatheroffice.gc.ca) provided by Environment Canada. The variables

required by the Prairie Blowing Snow Model (PBSM) (Pomeroy and Li, 2000) in the Cold Regions Hydrological Modelling platform (CRHM) include air temperature (t, °C), relative humidity (rh, %), wind speed (u, m/s), precipitation (p, mm). All variables were downloaded in hourly increments with the exception of precipitation data, for which only daily data was available. The incoming shortwave radiation (Q_{si}, W/m^2) is not needed to run the PBSM, but for a multi-year simulation of winter snow accumulation in CRHM, the energy-budget balance model (EBSM) (Gray and Landine, 1988) is required to melt the seasonal snow accumulation. However, the hourly incoming shortwave radiation is not observed at both stations and was estimated by a simple method presented by Annandale et al. (2002) as described by Shook and Pomeroy (2011).

Raw data from February 1994 to April 2011 was downloaded from the Rosetown East station and from August 1996 to April 2011 from the Outlook PFRA station. The quality of the raw data was checked and missing data gaps were filled using different interpolation techniques. If the missing gaps were of a relatively long period, more than one week, then a spatial interpolation technique was applied. This technique involved developing correlation equations between observations at the Rosetown East and the Outlook PFRA stations and applying these equations to estimated missing data. In regards to the Rosetown East station when dealing with precipitation data, another station – the main Rosetown station was used during its provided period from 1993 to 2000; having this station available allowed for more accurate precipitation interpolations over these years. In the cases of data missing from both Rosetown East and the Outlook PFRA stations, data from the Environment Canada station located at Elbow, Saskatchewan were used in estimating missing data at the Outlook PFRA station based on developed station correlation between Elbow and Outlook; missing data at the Rosetown East station was estimated using observations from Environment Canada's station at Lucky Lake, Saskatchewan using station correlation between Lucky Lake and Rosetown. A temporal averaging interpolation technique was used to fill data gaps that were less than two days. This method involved averaging the available data three days before the missing data gap along with the data three days after the missing gap to produce hourly estimates.

In addition to the missing data gaps, an error was found for the precipitation collected at the Outlook PFRA station in 2011. Hence, a comparison of annual precipitation between the Rosetown East and Outlook PFRA stations was carried out, and a double-mass curve between the two stations was derived based on the accumulated annual precipitation during 1996 to 2010 at both stations (Figure 3). Moreover, a correlation equation for the double-mass curve was generated (Equation 1) and used to interpolate the precipiation at Outlook in 2011.

$$p[Outlook] = 1.0826\,p[Rosetown] \qquad r^2 = 0.9965 \qquad [1]$$

After the data quality checking process, the hourly air temperature, relative humidity, wind speed, and incoming shortwave radiation and daily precipiation at the Outlook PFRA station was formatted to CRHM observation data files formats (.obs) from 1 October 1996 to 14 April 2011. The reason for using data from the Outlook station is for its close proximity to the shelterbelt sites at the Conquest.

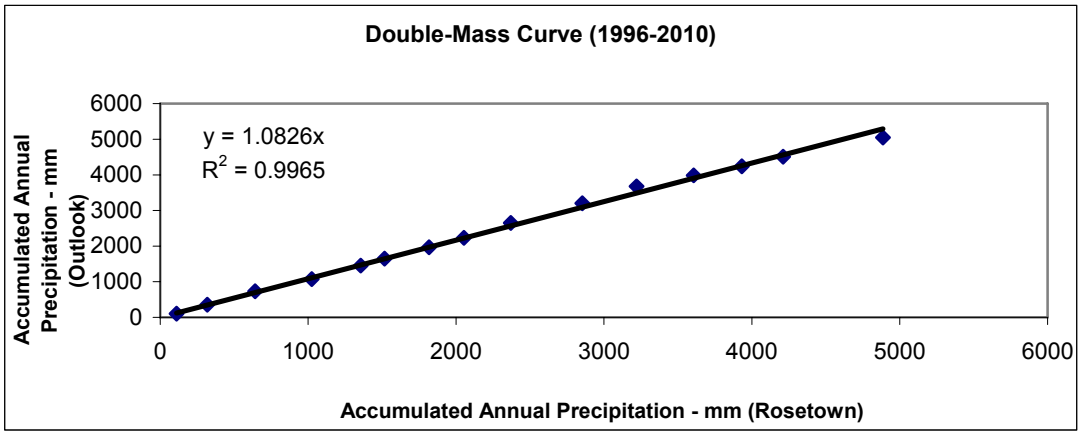

Figure 3. Double-mass curve of the accumulated annual precipiation between Outlook and Rosetown.

2.2.2 Field Observation Data

To evaluate the model's performance for snow accumulation at the shelterbelt sites, snow surveys of depth and density were conducted along three transects at the narrowly spaced shelterbelt site on 21 and 22 February 2011 shown in Figure 2(b) and along three transects at the widely spaced shelterbelt site on 23 February 2011 shown in Figure 2(a). Snow depth was measured using a metal ruler at 1-m interval along the transects. The snow density measurement was done at variable spacing in the field, with three collections for the shelterbelt at 2, 5 and 10 m from the centre of shelterbelt and one measurement for the open field in the middle of the field. The tare of snow tube (W_{tare}, in g) and weight of snow tube with snow sample (W_{snow}, in g) were measured and used with snow depth (d, in cm) to calculate snow density (ρ, in g/cm^3) based on the following equation:

$$\rho = \frac{W_{snow} - W_{tare}}{d} \qquad [2]$$

Both snow depth and density (ρ, in g/cm^3) measurements were used to calculate the snow accumulation (SWE, in mm):

$$SWE = 10 * d * \rho_{ave} \qquad [3]$$

3 Model Structure and Parameterization

3.1. Model Structure

The Cold Regions Hydrological Model platform (CRHM) was used to develop a shelterbelt model to simulate snow accumulation influenced by the surface roughness of shelterbelts and the surrounding crop fields at the Conquest. CRHM (Pomeroy et al., 2007) is an object-oriented, modular and flexible platform for assembling physically based hydrological models. With CRHM, the user constructs a purpose-built model or "project", from a selection of possible basin spatial configurations, spatial resolutions, and physical process modules of varying degrees of physical complexity. The hydrological processes are simulated on landscape units called hydrological response units (HRU). HRUs are defined as spatial units of mass and energy balance calculation corresponding to hydrobiophysical landscape units, within which processes and states are represented by single sets of parameters, state variables, and fluxes. Physically-based models are chosen depending on the dominant hydrological processes and controls on the basin.

A set of physically based modules was linked in a sequential fashion to simulate the snow accumulation at Conquest shelterbelt sites. Figure 4 shows the schematic of these modules, and these modules include:

1. Observation module: reads the meteorological data (temperature, wind speed, relative humidity, precipitation, and radiation), providing these inputs to other modules.
2. Garnier and Ohmura's radiation module (Garnier and Ohmura, 1970): calculates the theoretical global radiation, direct and diffuse solar radiation, as well as maximum sunshine hours based on latitude, elevation, ground slope, and azimuth, providing radiation inputs to sunshine hour module, energy-budget snowmelt module, net all-wave radiation module.
3. Sunshine hour module: estimates sunshine hours from incoming short-wave radiation and maximum sunshine hours, generating inputs to energy-budget snowmelt module, net all-wave radiation module.
4. Gray and Landine's albedo module (Gray and Landine, 1987): estimates snow albedo throughout the winter and into the melt period and indicates the beginning of melt for the energy-budget snowmelt module;
5. PBSM module or Prairie Blowing Snow Model (Pomeroy and Li, 2000): simulates the wind redistribution of snow and estimates snow accumulation and density changes throughout the winter period. This is the key module for the shelterbelt model.
6. EBSM module or Energy-Budget Snowmelt Model (Gray and Landine, 1988): estimates snowmelt by calculating the energy balance of radiation, sensible heat, latent heat, ground heat, advection from rainfall, and change in internal energy. This module is not necessary for simulating winter snow accumulation, but it is required in melt snow in the multi-year simulation such as the 15-year shelterbelt scenario simulation.

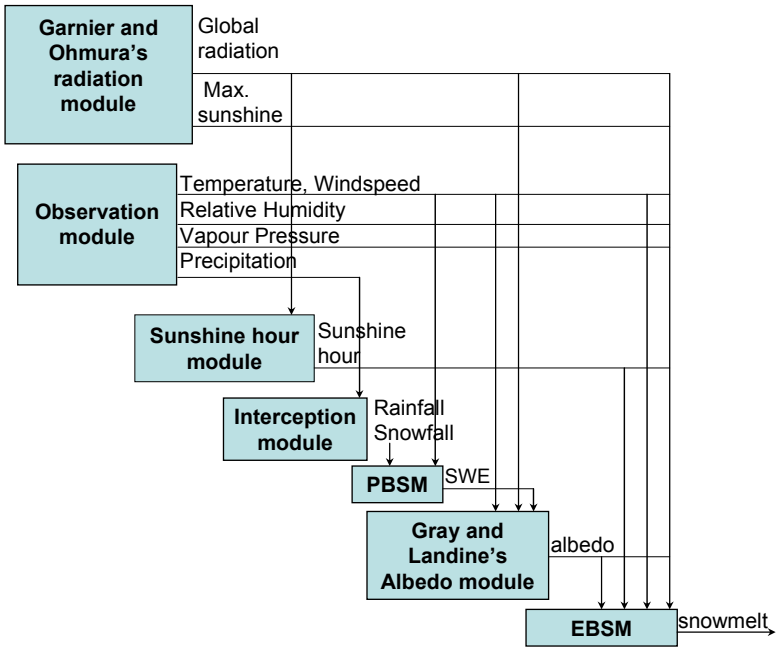

Figure 3. Flowchart of physically based hydrological modules for the shelterbelt model.

3.2. Model Parameterization

Three and seven HRUs were set up for the shelterbelt model at the widely and narrowly spaced shelterbelt sites, respectively. The number of HRUs was determined by the number of the crop fields and shelterbelts at each site shown in Figure 2. Key parameters used for simulating snow accumulation by the PBSM include area, vegetation height, blowing snow fetch distance and blowing snow distribution parameter; other essential parameters are latitude, elevation, and vegetation type. Table 1 shows the values for these parameters at both shelterbelt sites.

Table 1. Parameters for the shelterbelt model at Conquest, SK.

HRU Name	Area (km^2)	Vegetation Height (m)	Vegetation Type	Blowing Snow Fetch (m)	Latitude (°)	Elevation (m)	Blowing Snow Distribution Parameter
Conquest Narrowly Spaced Shelterbelt Site - Jay Spence							
Open Field 1	0.32	0.01	Lentil stubble	300	51.53	538	1
Shelterbelt 2	0.032	4.5	Caragana	300	51.53	538	-5
Open Field 2	0.88	0.01	Lentil stubble	1000	51.53	537	1
Shelterbelt 3	0.032	20	Elms/Caragana mix	500	51.53	532	-5
Open Field 3	0.2128	0.3	Wheat stubble	300	51.53	531	1
Shelterbelt 4	0.032	10	Elms/Caragana mix	300	51.53	530	-5
Open Field 4	0.2128	0.2	Wheat stubble	300	51.53	529	1
Conquest Widely Spaced Shelterbelt Site - Van Ray							
Open Field 1	0.64	0.01	Wheat stubble	1000	51.56	549	1
Shelterbelt	0.016	5	Caragana	800	51.56	549	-5
Open Field 2	0.64	0.01	Wheat stubble	1000	51.56	547	1

The area for open crop field HRU was estimated based on the dimensions shown in Figure 2; the effective width for the shelterbelt HRU was set as 20 m and was multiplied with the length shown in Figure 2 to calculate the area for shelterbelt HRU. Vegetation height and type were observed in the field. Blowing snow fetch distance was determined based on the dimensions shown in Figure 2, and minimum 300 m used by the PBSM was set if the distance was shorter than 300 m. The blowing snow distribution parameter was decided based on the surface roughness, with the value of 1 for cropped fields that could be source areas for blowing snow; the negative value for the shelterbelt HRU forces all snow transport to be captured by shelterbelt as is normal for a sink area. The source and sink area concept is discussed by Pomeroy et al (1998) and the blowing snow distribution parameter is described by Fang and Pomeroy (2009) and MacDonald et al. (2009).

4. Model Evaluation

The winter snowpack at both Conquest narrowly spaced (narrow) and widely spaced (wide) shelterbelt sites was simulated for the period 1 October 2010 to 14 April 2011 by the shelterbelt model. The model estimated snow depth (in cm) and snow accumulation (in mm water equivalent) were compared to the observed snow depth and accumulation at the narrow shelterbelt site on 22 February 2011 (Figure 4) and at the wide shelterbelt site on 23 February 2011 (Figure 5). Both figures show differences between the model simulation and field measurement of snow depth and snow accumulation. Larger differences are generally found in snow depth compared to snow accumulation suggesting the model is better at estimating snow mass balance than estimating depth in the field. This is in accordance with the model's design as a hydrological model focused on the water (mass) balance. In addition, when comparing to the measurements, the model had better estimates for both shelterbelts 2 and 3 at the narrow site and the shelterbelt at the wide site than for snow accumulation in the open fields.

The modelled snow depth and snow accumulation are plotted against the eight measured snow depth and eight measured snow accumulation surveys from both narrow and wide shelterbelt sites in Figure 6. The results show that the modelled snow depth and snow accumulation have a closer agreement with the measurements for deeper snow (i.e. snow depth > 70 cm or snow accumulation > 200 mm), which occurred at the shelterbelts. This implies better estimation for the shelterbelts than for the open fields. A statistical index, root mean square difference (RMSD), was calculated (Equation 4) and was used to assess the model's overall performance at both narrow and wide shelterbelt sites.

$$RMSD = \frac{1}{n}\sqrt{\sum_{i=1}^{n}(Modelled_i - Measured_i)^2} \qquad [4]$$

The RMSD values are 6.2 cm and 16.1 mm for the modelled snow depth and snow accumulation which are considered acceptable for modelling purposes.

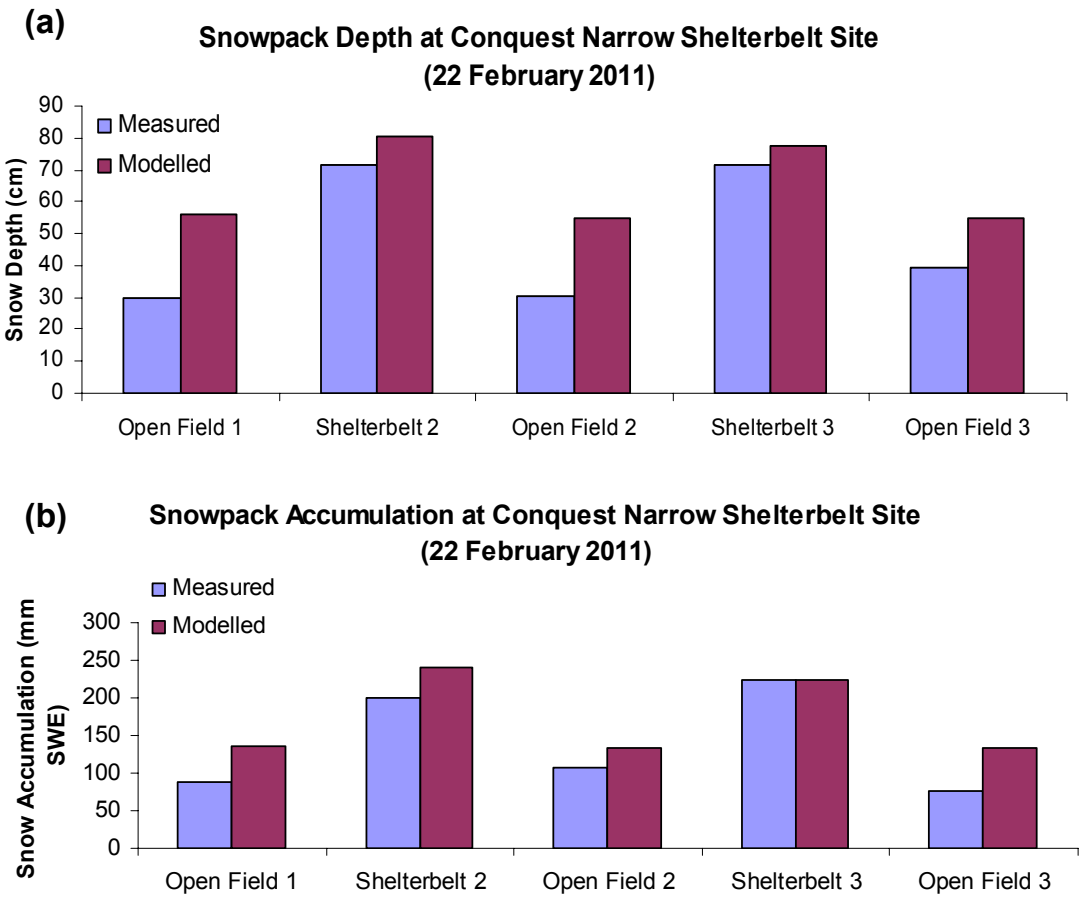

Figure 4. Comparison of modelled and measured snow depth and snow accumulation at the Conquest narrowly spaced (narrow) shelterbelt site on 22 February 2011.

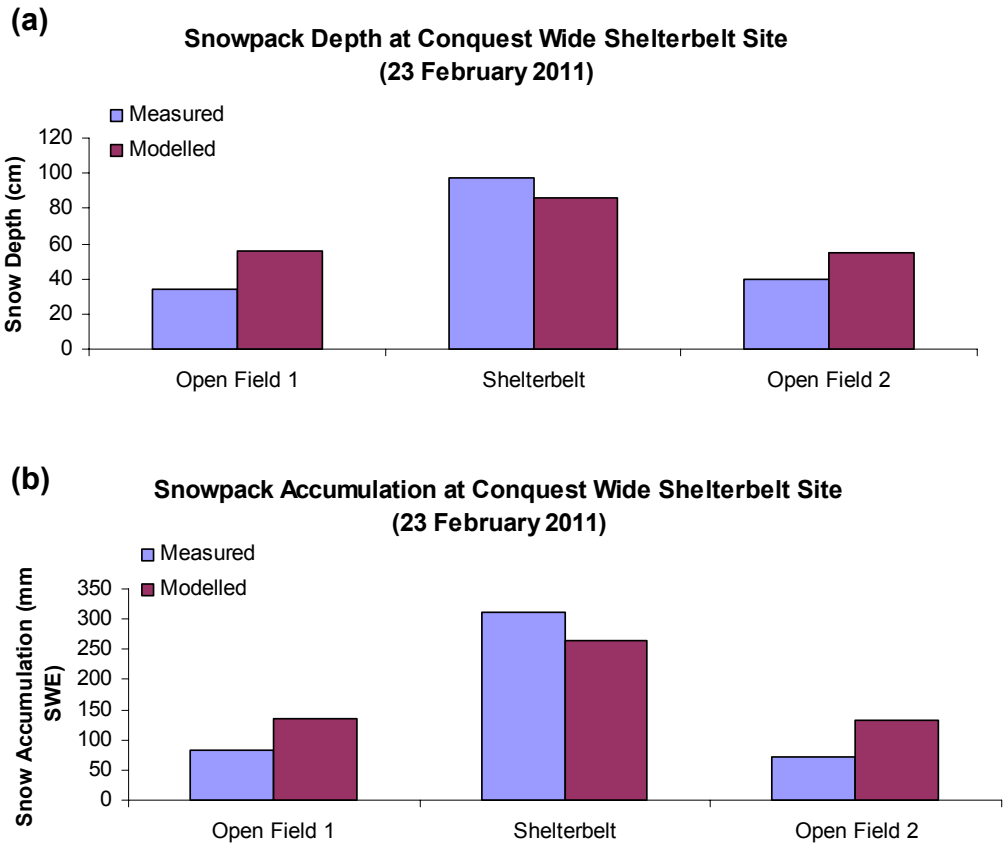

Figure 5. Comparison of modelled and measured snow depth and snow accumulation at the Conquest wide shelterbelt site on 22 February 2011.

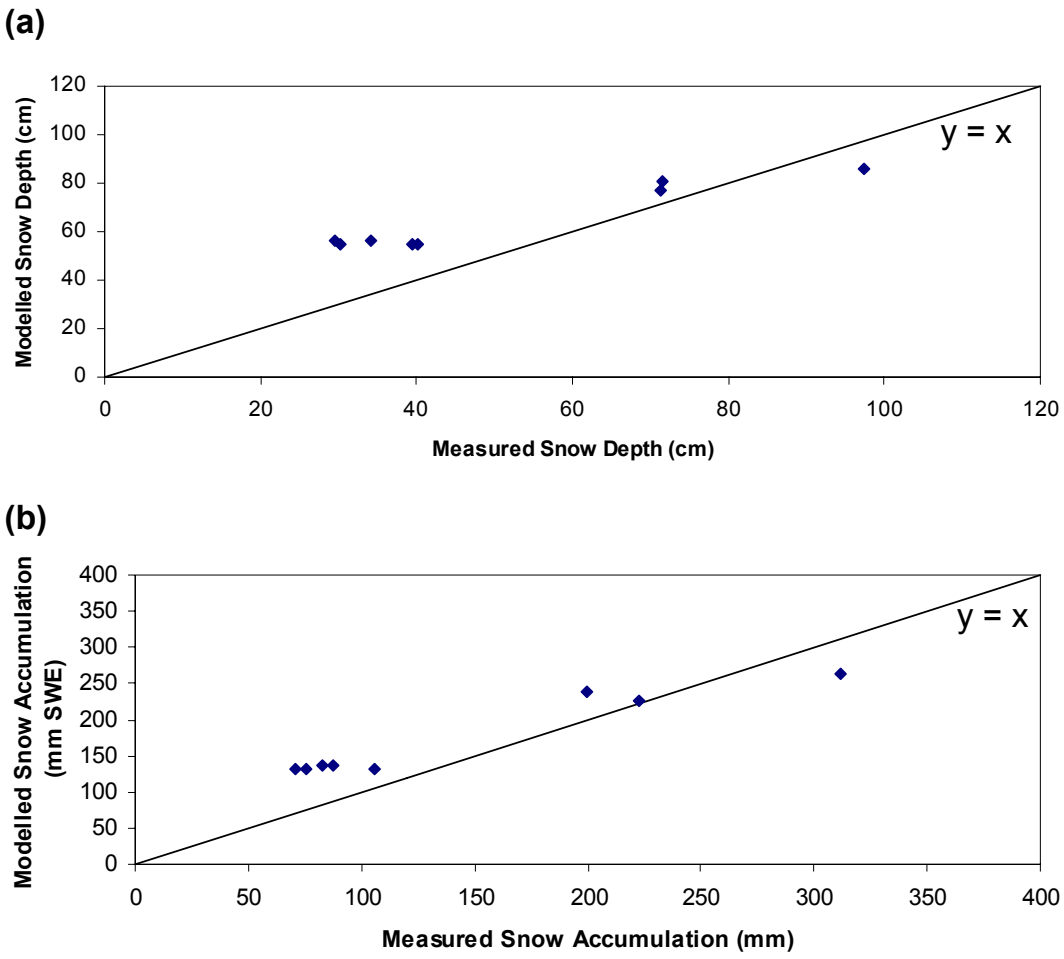

Figure 6. Comparison between the modelled and measured snow depth and snow accumulation.

Figures 4 to 6 demonstrate that the shelterbelt model has some predictability for snow accumulation at shelterbelts and is less accurate for the open crop fields, while the overall performance measured by the RMSD is fairly reasonable. It should be noted that this model performance evaluation is solely based on one-day comparison with the field measurements, and it is difficult to draw a conclusion on the model performance over the entire winter season. The one-day comparison should be treated with caution and simply as a model performance demonstration. It should be noted that PBSM is the key model used in the shelterbelt model, and its capability for predicting snow accumulation over full winter seasons has been shown in various open environments (Pomeroy et al., 1993; Pomeroy and Li, 2000; Fang and Pomeroy, 2007; Fang and Pomeroy, 2009; MacDonald et al., 2009; Fang et al., 2010).

5. Shelterbelt Scenarios Modelling

5.1. Scenario Description

A virtual half section land, 1.28 km^2 in total area and located in Conquest area, was chosen for developing various shelterbelt scenarios. Eleven scenarios of virtual shelterbelts were developed and range from no shelterbelt, a single shelterbelt to several shelterbelts with various spacing distances. Table 2 summarizes the description of these shelterbelt scenarios. The detailed configuration of spacing between the shelterbelts as well as the dimensions for the crop fields is depicted in Figures 7 to 17.

Table 2. Description of 11 shelterbelt scenarios.

Scenario Number	Description
1	Two crop fields with no shelterbelt
2	Two crop fields with a single shelterbelt
3	Three crop fields with two shelterbelts
4	Four crop fields with three shelterbelts
5	Four crop fields with four shelterbelts
6	Five crop fields with four shelterbelts
7	Five crop fields with five shelterbelts
8	Six crop fields with five shelterbelts
9	Six crop fields with six shelterbelts
10	Eight crop fields with seven shelterbelts
11	Eight crop fields with eight shelterbelts

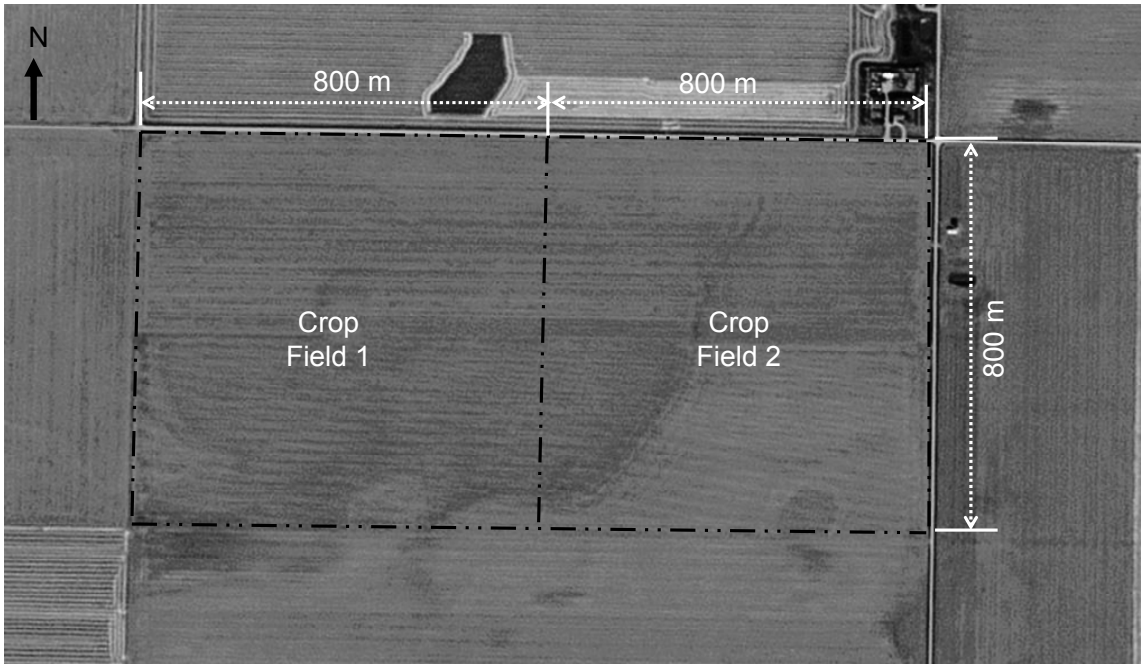

Figure 7. Virtual site configuration for the shelterbelt scenario 1.

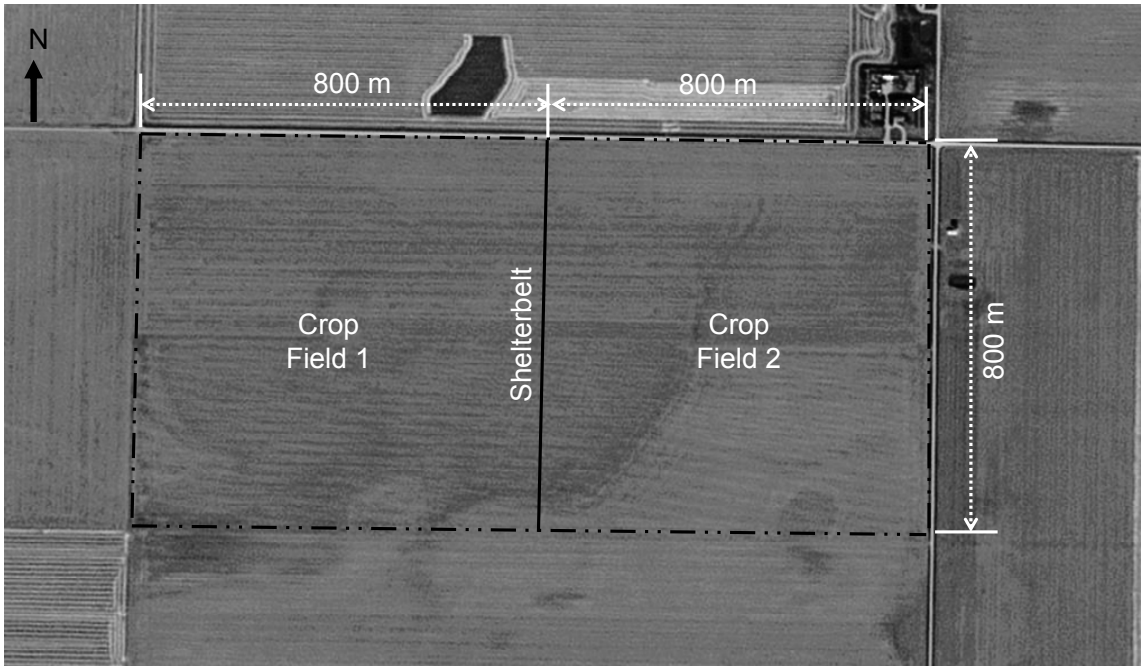

Figure 8. Virtual site configuration for the shelterbelt scenario 2.

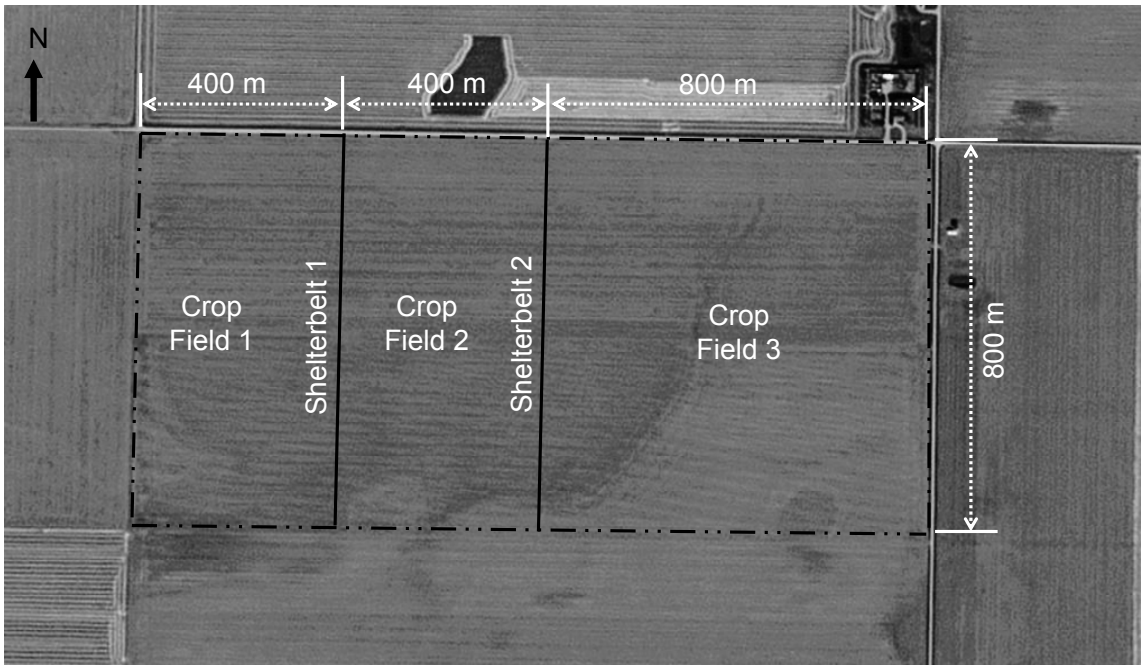

Figure 9. Virtual site configuration for the shelterbelt scenario 3.

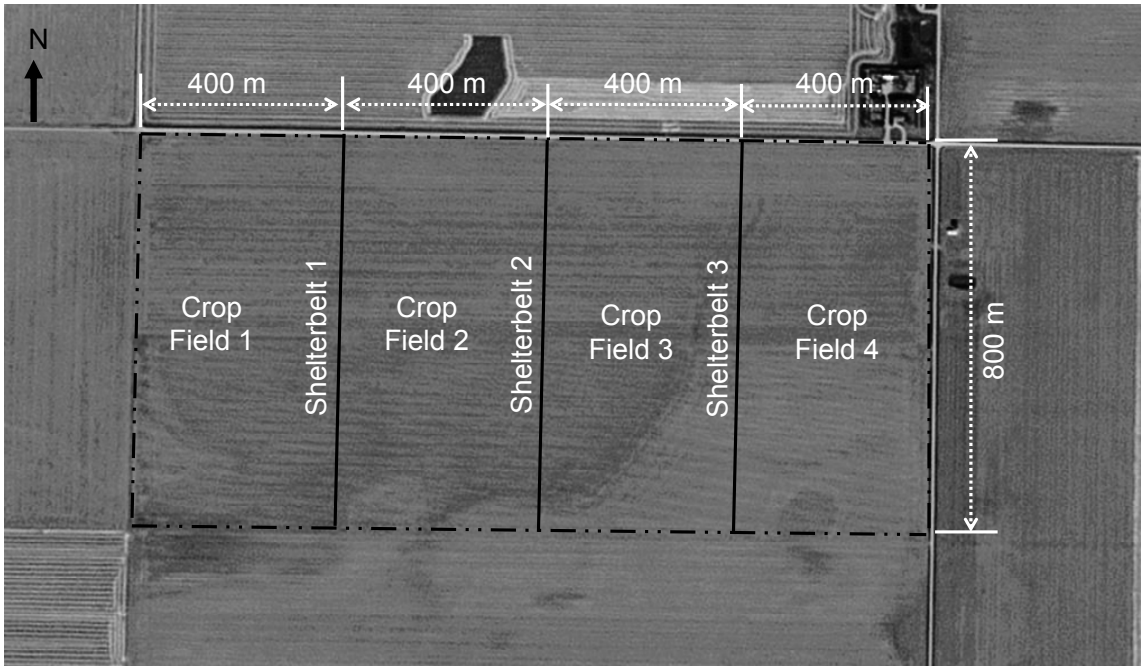

Figure 10. Virtual site configuration for the shelterbelt scenario 4.

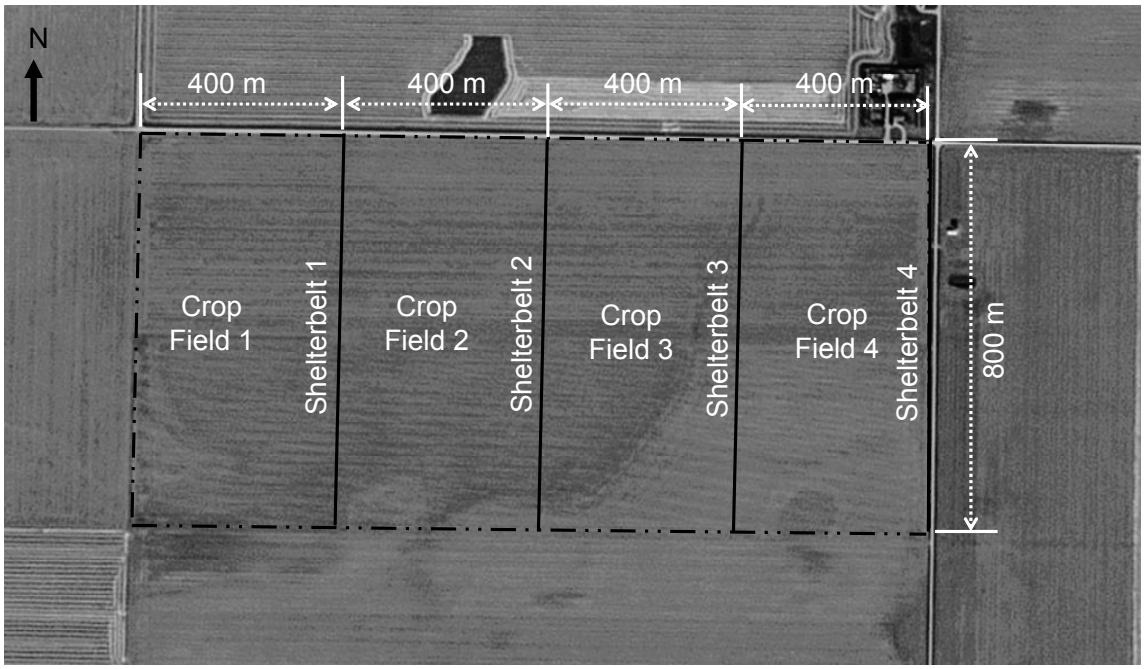

Figure 11. Virtual site configuration for the shelterbelt scenario 5.

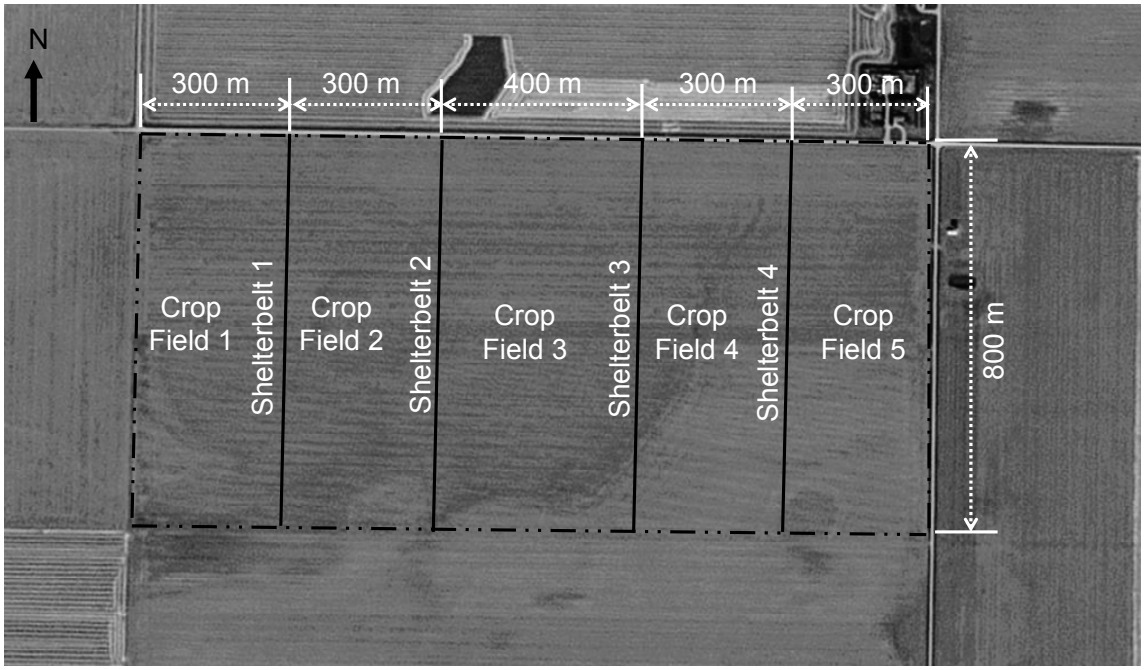

Figure 12. Virtual site configuration for the shelterbelt scenario 6.

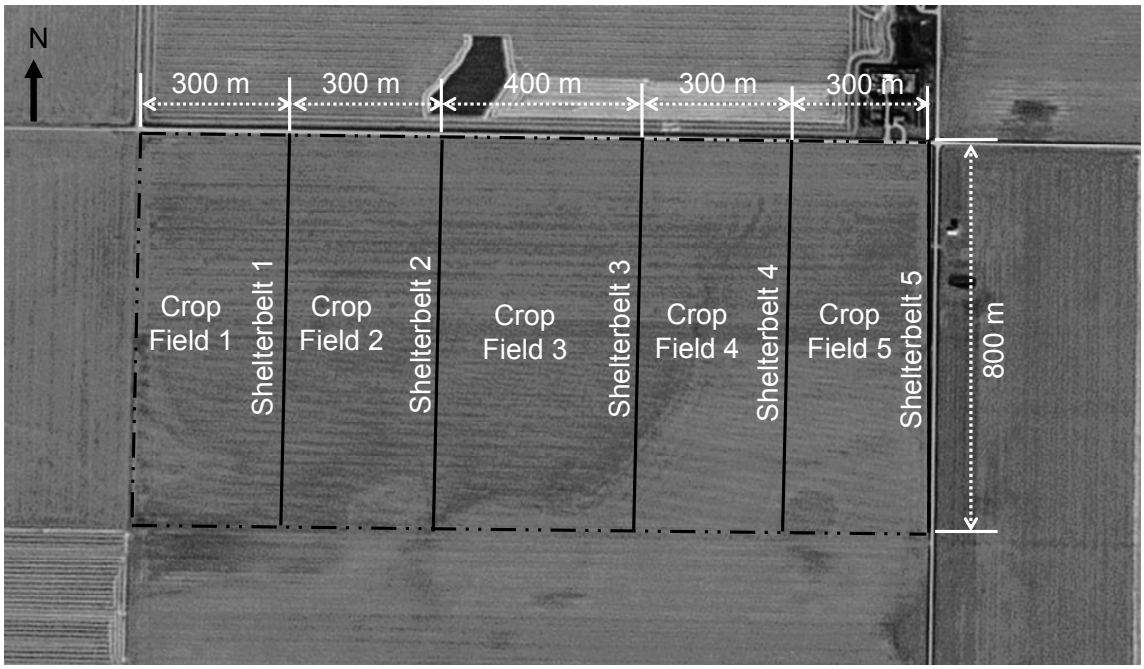

Figure 13. Virtual site configuration for the shelterbelt scenario 7.

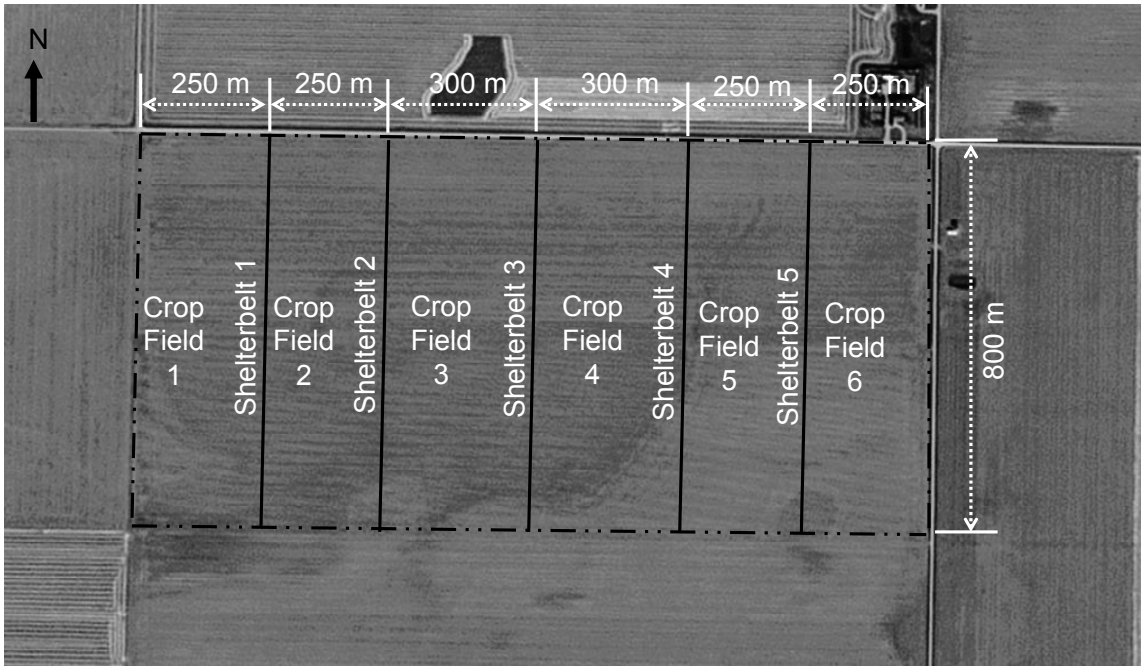

Figure 14. Virtual site configuration for the shelterbelt scenario 8.

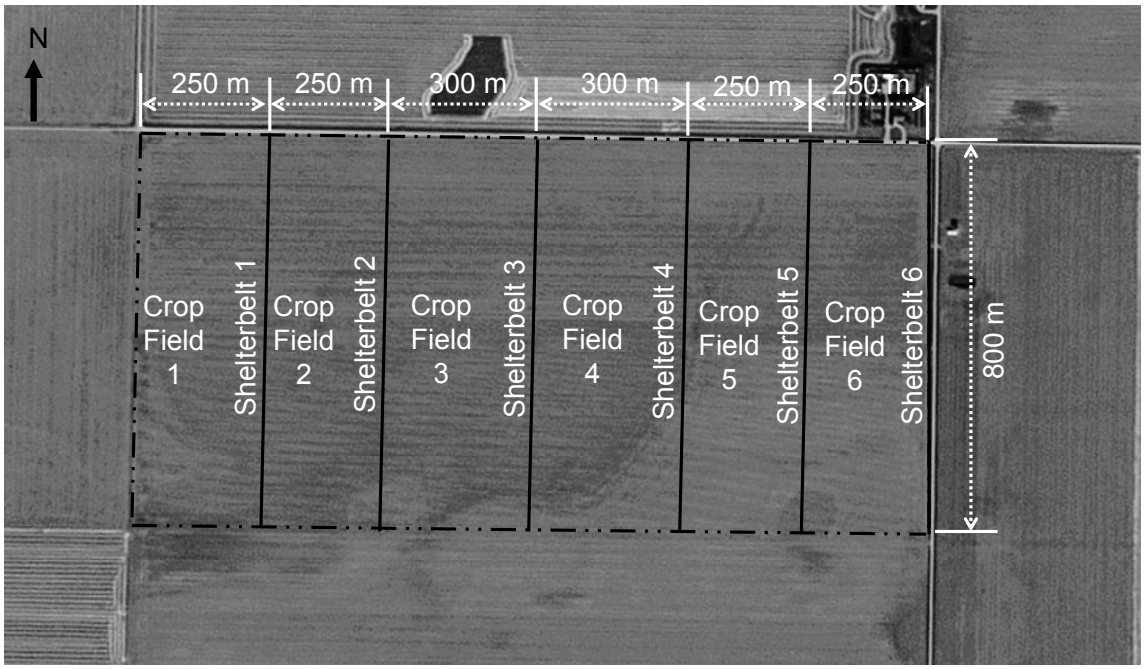

Figure 15. Virtual site configuration for the shelterbelt scenario 9.

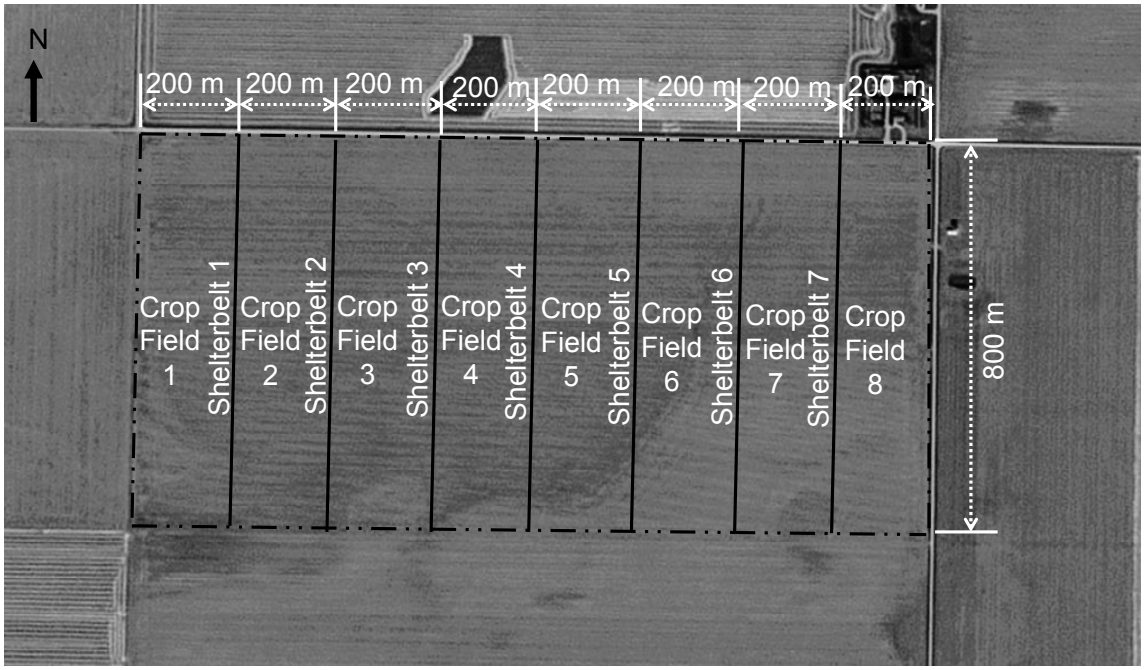

Figure 16. Virtual site configuration for the shelterbelt scenario 10.

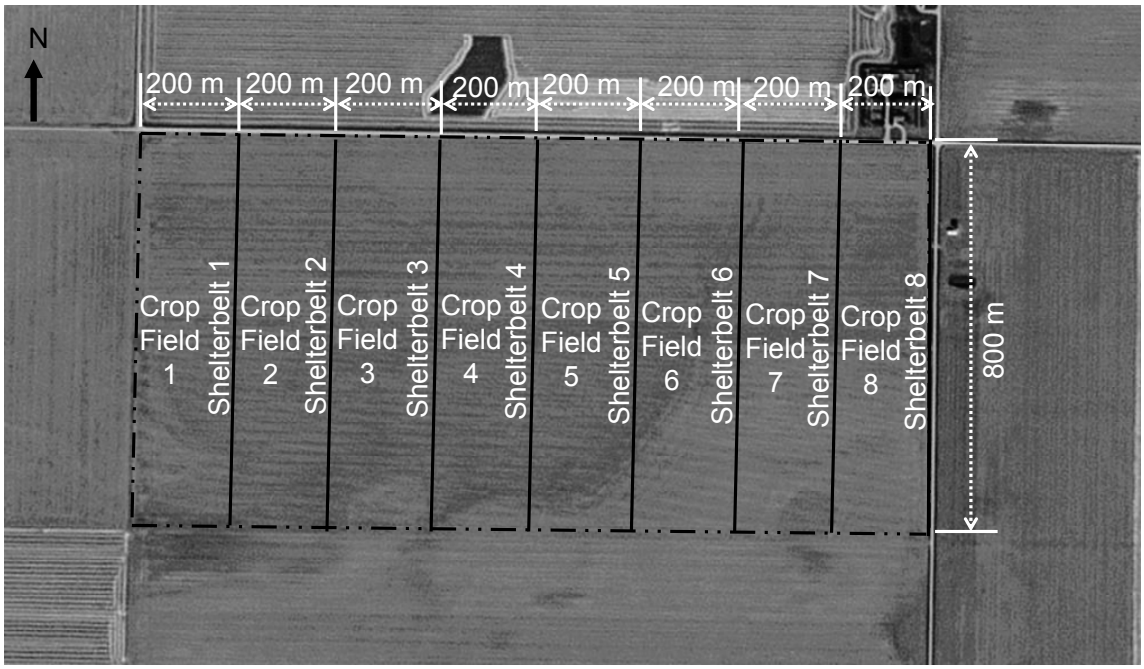

Figure 17. Virtual site configuration for the shelterbelt scenario 11.

The shelterbelt model described in the previous section was used in 15-year (1996-2011) simulation using the cleaned historical data of air temperature, relative humidity, wind speed, incoming shortwave radiation, and precipitation from Outlook PFRA station. The 15-year continues simulations were conducted for all 11 shelterbelt scenarios based on key parameters listed in Tables 3 to 13.

Table 3. Parameters for the shelterbelt model in the scenario 1.

HRU	Area (km^2)	Vegetation Height (m)	Vegetation Type	Blowing Snow Fetch (m)	Latitude (°)	Elevation (m)	Blowing Snow Distribution Parameter
Crop Field 1	0.64	0.15	Wheat Stubble	1500	51.56	549	1
Crop Field 2	0.64	0.15	Wheat Stubble	1500	51.56	547	2

Table 4. Parameters for the shelterbelt model in the scenario 2.

HRU	Area (km^2)	Vegetation Height (m)	Vegetation Type	Blowing Snow Fetch (m)	Latitude (°)	Elevation (m)	Blowing Snow Distribution Parameter
Crop Field 1	0.632	0.15	Wheat stubble	1000	51.56	549	1
Shelterbelt	0.016	5	Caragana belt	800	51.56	549	-5
Crop Field 2	0.632	0.15	Wheat stubble	1000	51.56	547	1

Table 5. Parameters for the shelterbelt model in the scenario 3.

HRU	Area (km^2)	Vegetation Height (m)	Vegetation Type	Blowing Snow Fetch (m)	Latitude (°)	Elevation (m)	Blowing Snow Distribution Parameter
Crop Field 1	0.312	0.15	Wheat stubble	600	51.56	549	1
Shelterbelt 1	0.016	5	Caragana belt	400	51.56	549	-5
Crop Field 2	0.304	0.15	Wheat stubble	600	51.56	549	1
Shelterbelt 2	0.016	5	Caragana belt	400	51.56	549	-5
Crop Field 3	0.632	0.15	Wheat stubble	1000	51.56	548	1

Table 6. Parameters for the shelterbelt model in the scenario 4.

HRU	Area (km^2)	Vegetation Height (m)	Vegetation Type	Blowing Snow Fetch (m)	Latitude (°)	Elevation (m)	Blowing Snow Distribution Parameter
Crop Field 1	0.312	0.15	Wheat stubble	600	51.56	549	1
Shelterbelt 1	0.016	5	Caragana belt	400	51.56	549	-5
Crop Field 2	0.304	0.15	Wheat stubble	600	51.56	549	1
Shelterbelt 2	0.016	5	Caragana belt	400	51.56	549	-5
Crop Field 3	0.304	0.15	Wheat stubble	600	51.56	548	1
Shelterbelt 3	0.016	5	Caragana belt	400	51.56	548	-5
Crop Field 4	0.312	0.15	Wheat stubble	600	51.56	547	1

Table 7. Parameters for the shelterbelt model in the scenario 5.

HRU	Area (km^2)	Vegetation Height (m)	Vegetation Type	Blowing Snow Fetch (m)	Latitude (°)	Elevation (m)	Blowing Snow Distribution Parameter
Crop Field 1	0.312	0.15	Wheat stubble	600	51.56	549	1
Shelterbelt 1	0.016	5	Caragana belt	400	51.56	549	-5
Crop Field 2	0.304	0.15	Wheat stubble	600	51.56	549	1
Shelterbelt 2	0.016	5	Caragana belt	400	51.56	549	-5
Crop Field 3	0.304	0.15	Wheat stubble	600	51.56	548	1
Shelterbelt 3	0.016	5	Caragana belt	400	51.56	548	-5
Crop Field 4	0.296	0.15	Wheat stubble	600	51.56	547	1
Shelterbelt 4	0.016	5	Caragana belt	400	51.56	547	-5

Table 8. Parameters for the shelterbelt model in the scenario 6.

HRU	Area (km^2)	Vegetation Height (m)	Vegetation Type	Blowing Snow Fetch (m)	Latitude (°)	Elevation (m)	Blowing Snow Distribution Parameter
Crop Field 1	0.232	0.15	Wheat stubble	450	51.56	549	1
Shelterbelt 1	0.016	5	Caragana belt	300	51.56	549	-5
Crop Field 2	0.224	0.15	Wheat stubble	450	51.56	549	1
Shelterbelt 2	0.016	5	Caragana belt	300	51.56	549	-5
Crop Field 3	0.304	0.15	Wheat stubble	600	51.56	548	1
Shelterbelt 3	0.016	5	Caragana belt	400	51.56	548	-5
Crop Field 4	0.224	0.15	Wheat stubble	450	51.56	547	1
Shelterbelt 4	0.016	5	Caragana belt	300	51.56	547	-5
Crop Field 5	0.232	0.15	Wheat stubble	450	51.56	547	1

Table 9. Parameters for the shelterbelt model in the scenario 7.

HRU	Area (km^2)	Vegetation Height (m)	Vegetation Type	Blowing Snow Fetch (m)	Latitude (°)	Elevation (m)	Blowing Snow Distribution Parameter
Crop Field 1	0.232	0.15	Wheat stubble	450	51.56	549	1
Shelterbelt 1	0.016	5	Caragana belt	300	51.56	549	-5
Crop Field 2	0.224	0.15	Wheat stubble	450	51.56	549	1
Shelterbelt 2	0.016	5	Caragana belt	300	51.56	549	-5
Crop Field 3	0.304	0.15	Wheat stubble	600	51.56	548	1
Shelterbelt 3	0.016	5	Caragana belt	400	51.56	548	-5
Crop Field 4	0.224	0.15	Wheat stubble	450	51.56	547	1
Shelterbelt 4	0.016	5	Caragana belt	300	51.56	547	-5
Crop Field 5	0.216	0.15	Wheat stubble	450	51.56	547	1
Shelterbelt 5	0.016	5	Caragana belt	300	51.56	547	-5

Table 10. Parameters for the shelterbelt model in the scenario 8.

HRU	Area (km^2)	Vegetation Height (m)	Vegetation Type	Blowing Snow Fetch (m)	Latitude (°)	Elevation (m)	Blowing Snow Distribution Parameter
Crop Field 1	0.192	0.15	Wheat stubble	375	51.56	549	1
Shelterbelt 1	0.016	5	Caragana belt	*300*	51.56	549	-5
Crop Field 2	0.184	0.15	Wheat stubble	375	51.56	549	1
Shelterbelt 2	0.016	5	Caragana belt	*300*	51.56	549	-5
Crop Field 3	0.224	0.15	Wheat stubble	450	51.56	548	1
Shelterbelt 3	0.016	5	Caragana belt	300	51.56	548	-5
Crop Field 4	0.224	0.15	Wheat stubble	450	51.56	548	1
Shelterbelt 4	0.016	5	Caragana belt	300	51.56	547	-5
Crop Field 5	0.184	0.15	Wheat stubble	375	51.56	547	1
Shelterbelt 5	0.016	5	Caragana belt	*300*	51.56	547	-5
Crop Field 6	0.192	0.15	Wheat stubble	375	51.56	547	1

Table 11. Parameters for the shelterbelt model in the scenario 9.

HRU	Area (km^2)	Vegetation Height (m)	Vegetation Type	Blowing Snow Fetch (m)	Latitude (°)	Elevation (m)	Blowing Snow Distribution Parameter
Crop Field 1	0.192	0.15	Wheat stubble	375	51.56	549	1
Shelterbelt 1	0.016	5	Caragana belt	*300*	51.56	549	-5
Crop Field 2	0.184	0.15	Wheat stubble	375	51.56	549	1
Shelterbelt 2	0.016	5	Caragana belt	*300*	51.56	549	-5
Crop Field 3	0.224	0.15	Wheat stubble	450	51.56	548	1
Shelterbelt 3	0.016	5	Caragana belt	300	51.56	548	-5
Crop Field 4	0.224	0.15	Wheat stubble	450	51.56	548	1
Shelterbelt 4	0.016	5	Caragana belt	300	51.56	547	-5
Crop Field 5	0.184	0.15	Wheat stubble	375	51.56	547	1
Shelterbelt 5	0.016	5	Caragana belt	*300*	51.56	547	-5
Crop Field 6	0.176	0.15	Wheat stubble	375	51.56	547	1
Shelterbelt 6	0.016	5	Caragana belt	*300*	51.56	547	-5

Table 12. Parameters for the shelterbelt model in the scenario 10.

HRU	Area (km^2)	Vegetation Height (m)	Vegetation Type	Blowing Snow Fetch (m)	Latitude (°)	Elevation (m)	Blowing Snow Distribution Parameter
Crop Field 1	0.152	0.15	Wheat stubble	300	51.56	549	1
Shelterbelt 1	0.016	5	Caragana belt	*300*	51.56	549	-5
Crop Field 2	0.144	0.15	Wheat stubble	300	51.56	549	1
Shelterbelt 2	0.016	5	Caragana belt	*300*	51.56	549	-5
Crop Field 3	0.144	0.15	Wheat stubble	300	51.56	549	1
Shelterbelt 3	0.016	5	Caragana belt	*300*	51.56	548	-5
Crop Field 4	0.144	0.15	Wheat stubble	300	51.56	548	1
Shelterbelt 4	0.016	5	Caragana belt	*300*	51.56	548	-5
Crop Field 5	0.144	0.15	Wheat stubble	300	51.56	548	1
Shelterbelt 5	0.016	5	Caragana belt	*300*	51.56	548	-5
Crop Field 6	0.144	0.15	Wheat stubble	300	51.56	547	1
Shelterbelt 6	0.016	5	Caragana belt	*300*	51.56	547	-5
Crop Field 7	0.144	0.15	Wheat stubble	300	51.56	547	1
Shelterbelt 7	0.016	5	Caragana belt	*300*	51.56	547	-5
Crop Field 8	0.152	0.15	Wheat stubble	300	51.56	547	1

Table 13. Parameters for the shelterbelt model in the scenario 11.

HRU	Area (km^2)	Vegetation Height (m)	Vegetation Type	Blowing Snow Fetch (m)	Latitude (°)	Elevation (m)	Blowing Snow Distribution Parameter
Crop Field 1	0.152	0.15	Wheat stubble	300	51.56	549	1
Shelterbelt 1	0.016	5	Caragana belt	*300*	51.56	549	-5
Crop Field 2	0.144	0.15	Wheat stubble	300	51.56	549	1
Shelterbelt 2	0.016	5	Caragana belt	*300*	51.56	549	-5
Crop Field 3	0.144	0.15	Wheat stubble	300	51.56	549	1
Shelterbelt 3	0.016	5	Caragana belt	*300*	51.56	548	-5
Crop Field 4	0.144	0.15	Wheat stubble	300	51.56	548	1
Shelterbelt 4	0.016	5	Caragana belt	*300*	51.56	548	-5
Crop Field 5	0.144	0.15	Wheat stubble	300	51.56	548	1
Shelterbelt 5	0.016	5	Caragana belt	*300*	51.56	548	-5
Crop Field 6	0.144	0.15	Wheat stubble	300	51.56	547	1
Shelterbelt 6	0.016	5	Caragana belt	*300*	51.56	547	-5
Crop Field 7	0.144	0.15	Wheat stubble	300	51.56	547	1
Shelterbelt 7	0.016	5	Caragana belt	*300*	51.56	547	-5
Crop Field 8	0.136	0.15	Wheat stubble	300	51.56	547	1
Shelterbelt 8	0.016	5	Caragana belt	*300*	51.56	547	-5

5.2. Scenario Results

5.2.1 Snow Accumulation

The seasonal winter snow accumulation (SWE) on the open (crop) field and shelterbelt HRUs were estimated for the 15-year period. The area-weighted average SWE was calculated for the crop field, shelterbelt, and the entire half section land using the Equations 5 to 7. The area-weight average SWE is the actual amount of snow accumulation at crop field, shelterbelt, and the entire half section land.

For crop field: $$SWE(crop\_field) = \frac{\sum_{i=1}^{n1} SWE(crop\_field_i) \times Area(crop\_field_i)}{Area(crop\_field)} \quad [5]$$

For shelterbelt: $$SWE(shelterbelt) = \frac{\sum_{j=1}^{n2} SWE(shelterbelt_j) \times Area(shelbterbelt_j)}{Area(shelbterbelt)} \quad [6]$$

For half section land:

$$SWE(half\_\sec) = \frac{\sum_{i=1}^{n1} SWE(crop\_field_i) \times Area(crop\_field_i) + \sum_{j=1}^{n2} SWE(shelterbelt_j) \times Area(shelterbelt_j)}{Area(crop\_field) + Area(shelterbelt)} \quad [7]$$

where $SWE(crop\_field_i)$ and $SWE\ (shelterbelt_j)$ are the simulated SWE at crop field (i) and shelterbelt (j), and $Area(crop\_field_i)$ and $Area\ (shelterbelt_j)$ are the area at crop field (i) and shelterbelt (j), with i and j being the number of crop field and shelterbelt in each scenario. *n1* and *n2* are the total number of crop field and shelterbelt, respectively. *Area(crop_field)* and *Area (shelterbelt)* are the respective total area of crop field and shelterbelt in each scenario.

The simulated time-series of SWE for crop field, shelterbelt, and entire half section land is shown in Figure 18. The figure shows that SWE is most sensitive to the year to year changes in seasonal snowfall and melt conditions and much less sensitive to the presence and number of shelterbelts. SWE is less sensitive to the changes in the numbers of shelterbelts during dry years (i.e. 2002) when compared to the wet years (i.e. 1997, 1998, and 2006).

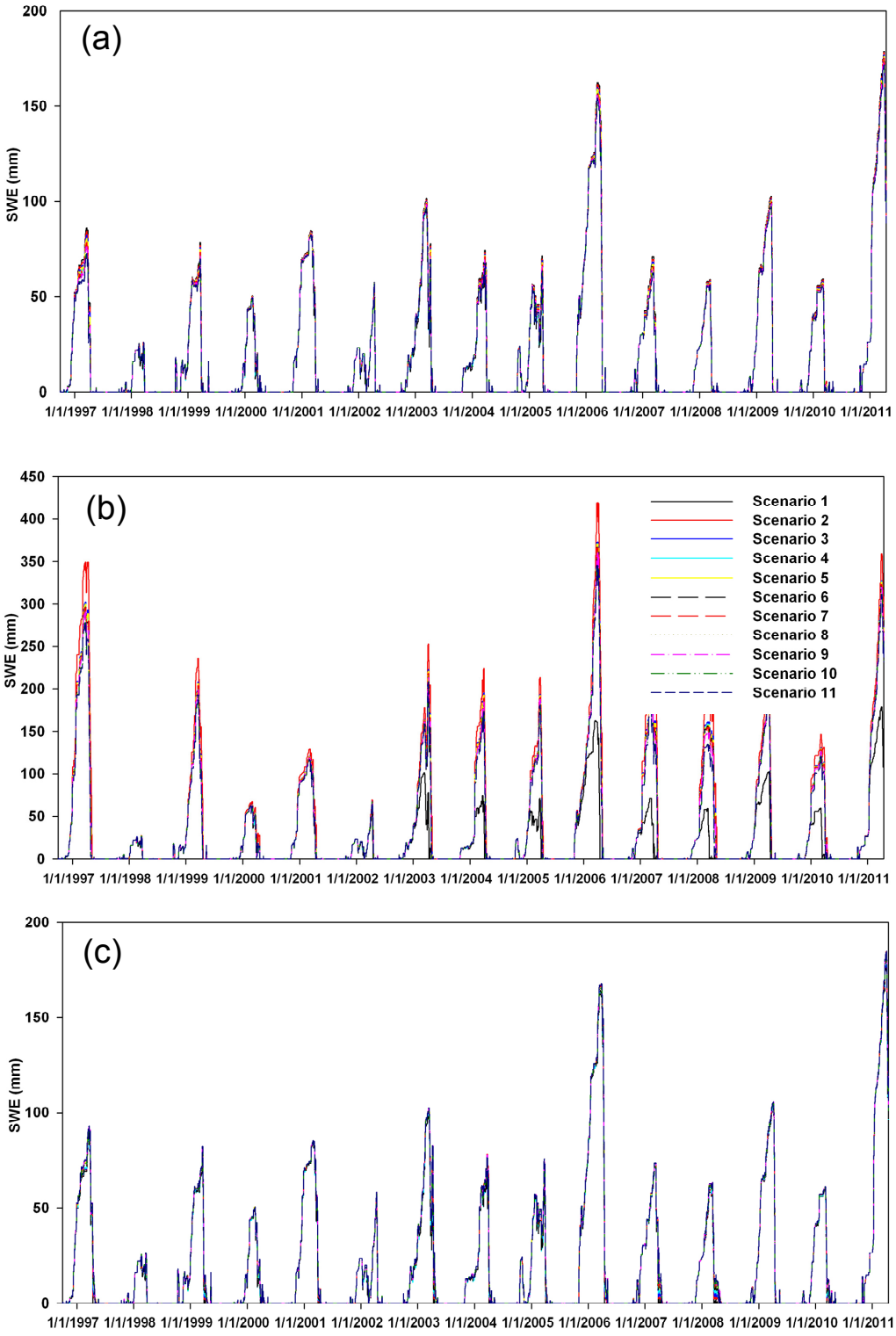

Figure 18. The simulated time-series of snow accumulation (SWE) during 15-year period (1 October 1996-14 April 2011) for the 11 shelterbelt scenarios. (a) Crop field, (b) shelterbelt, and (c) entire half section land.

The peak seasonal SWE was also calculated for crop field, shelterbelt, and the entire half section land during the 15-year period and is shown in Figure 19. . As the scenario proceeds from 1 to 11, the area of crop field steadily drops and area and number of shelterbelts gradually increases. The general trend of the peak SWE for crop land is to gradually decrease as the scenario proceeds from 1 to 11 and the number of shelterbelts increases. This is due to scour of fields to supply snow for wind transport downwind of the sheltering influence of the shelterbelts and capture of blowing snow by shelterbelts rather than stubble fields and is most pronounced in high snowfall seasons. The progression from scenario 2 to 11 generally leads to a decrease in the peak SWE for shelterbelts with the greatest decrease occurring in the snowiest seasons. This is due to the number of shelterbelts exceeding the available blowing snow transport to capture as drifts. It should be noted that the amount of snow retained over the half-section (peak SWE) increases with the number of shelterbelts, especially in the snowiest seasons. Figure 19 also illustrates that the peak SWE crop field, shelterbelt, and entire half section land for dry years (i.e. 1999-2000, 2000-2001) is less sensitive to the change in the numbers of crop field and shelterbelt in the scenarios compared to wet years (i.e. 2005-2006, 2010-2011).

In addition, the 15-year (1996-2011) averaged peak SWE was estimated for crop field, shelterbelt, and the entire half section land in each of 11 scenarios and is shown in Figure 20. The 15-year averaged peak SWE for the half section land in the scenarios 2 to 11 (i.e. half section land with various number of shelterbelts) was also compared to that in the scenario 1 (i.e. half section land with no shelterbelt), and this is shown in Figure 21 as "change in peak snow accumulation". Although the peak seasonal SWE for the shelterbelt is the largest in the scenario 2 show in Figure 20, that single shelterbelt occupies very little area (i.e. 0.016 km^2) in the entire half section land (1.28 km^2), and consequently it generates less than 1% of change in the peak SWE when compared to the scenario with no shelterbelt (Figure 21). Scenarios 5, 7, 9, and 11 result in greater increase in the peak SWE, ranging from 2 to 3 %, while scenarios 8 and 10 have slightly lower than 2% rise in peak SWE compared to the scenario 1. Scenarios 4 and 6 have smaller than 0.25% decrease in the peak SWE during 15-year period compared to the scenario 1. In general it can be stated that the presence of shelterbelts increases snow accumulation over the overall field, but there is no further benefit, on average, to adding more than four shelterbelts per half-section in this environment.

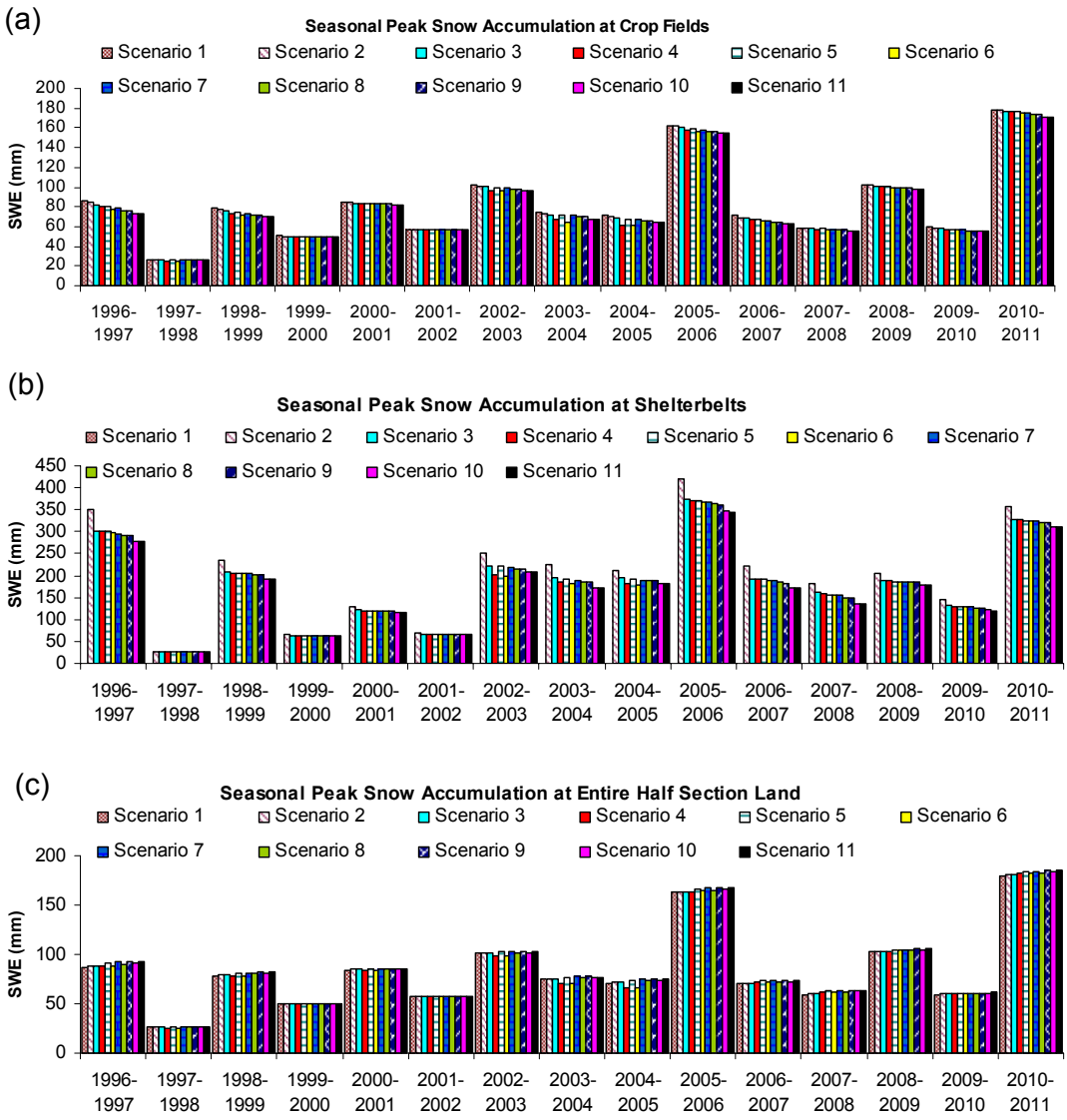

Figure 19. The simulated seasonal peak snow accumulation (SWE) during 15-year period (1 October 1996-14 April 2011) for the 11 shelterbelt scenarios. (a) Crop field, (b) shelterbelt, and (c) entire half section land.

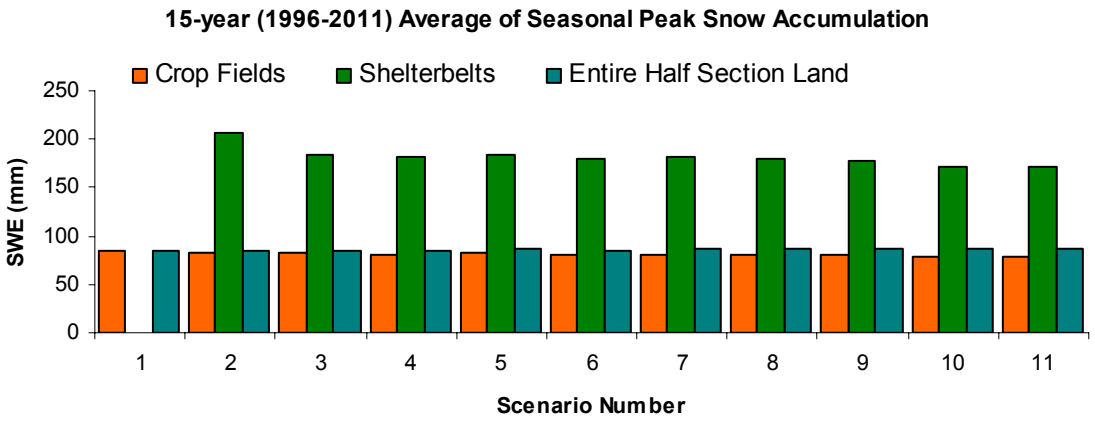

Figure 20. The 15-year (1996-2011) average of seasonal peak snow accumulation for the 11 scenarios.

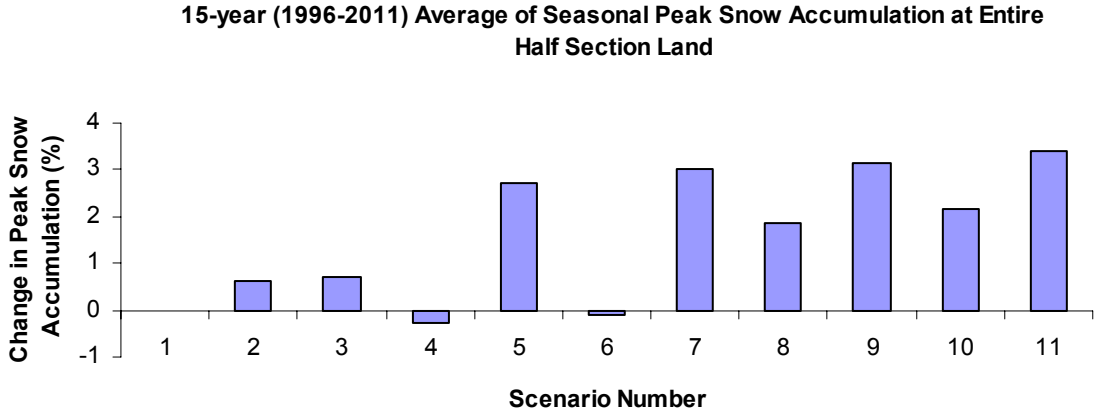

Figure 21. Change in the 15-year (1996-2011) average of seasonal peak snow accumulation. The change is the difference between the average seasonal peak snow accumulation in scenario 1 and other scenarios.

More analyses regarding the difference between the peak SWE in scenario 1 (i.e. half section land with no shelterbelt) and others scenarios (i.e. half section land with various number of shelterbelts) were taken in respect to the effect of seasonal snowfall and the results are shown in Figures 22 to 31. These figures illustrate the difference between the scenario 1 and other scenarios in terms of peak season SWE on the half section land under various seasonal snow accumulation conditions, ranging from dry seasons (i.e. peak SWE < 30 mm) to snowy seasons (i.e. peak SWE close to 180 mm). The difference in peak SWE is reflected in the change in the peak snow accumulation shown on the vertical axis of these figures. Generally, adding more shelterbelts has little or no effect on the peak SWE on the half section of land during dry conditions (i.e. peak SWE < 60 mm). For medium (i.e. 60 mm < peak SWE < 110 mm) and snowy (i.e. 160 mm < peak SWE < 180 mm) conditions, peak SWE on the half section of land generally increases with

increasing number of shelterbelts. The maximum change in the peak SWE on the half section land ranges from 1.6 mm in scenario 2 to 6.7 mm in scenario 11, corresponding to 2,048 m^3 and 8,576 m^3 more water on the half section land before snowmelt.

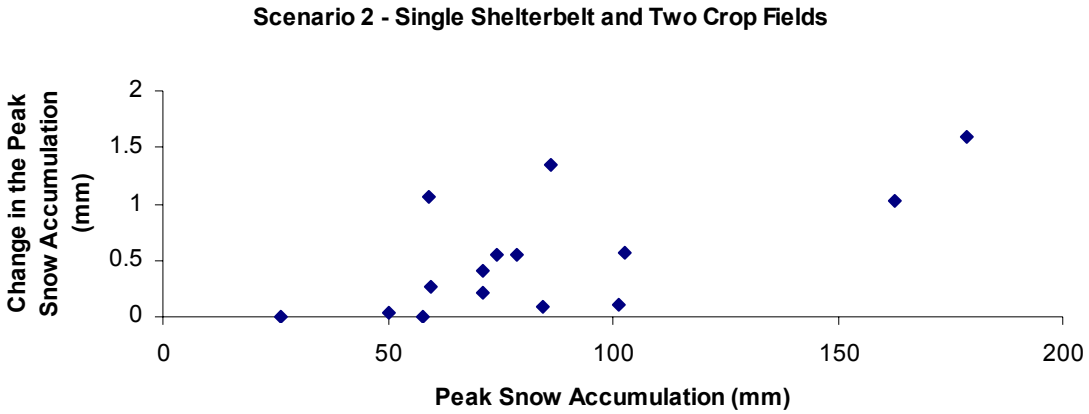

Figure 22. Change in the peak SWE in scenario 2 with respect to scenario 1.

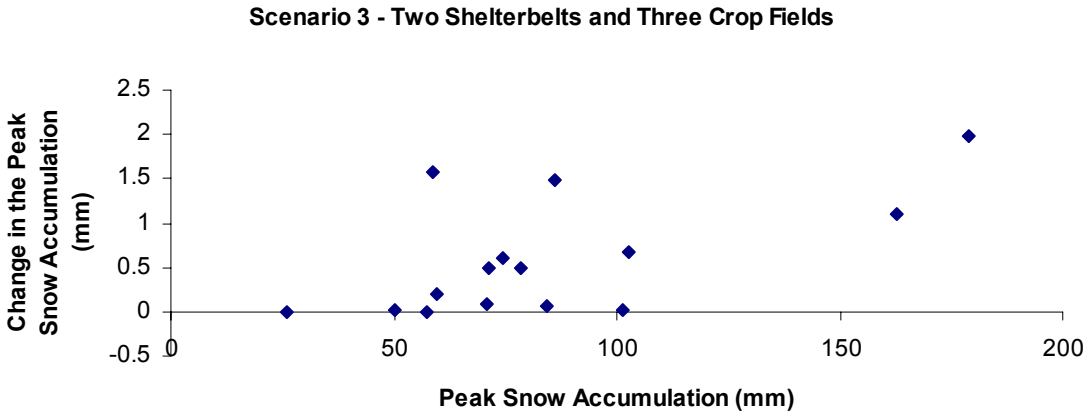

Figure 23. Change in the peak SWE in scenario 3 with respect to scenario 1.

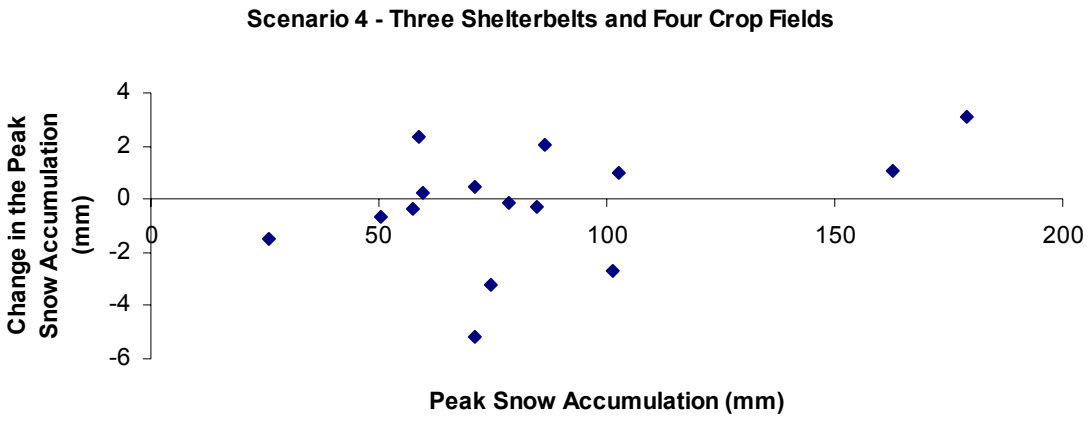

Figure 24. Change in the peak SWE in scenario 4 with respect to scenario 1.

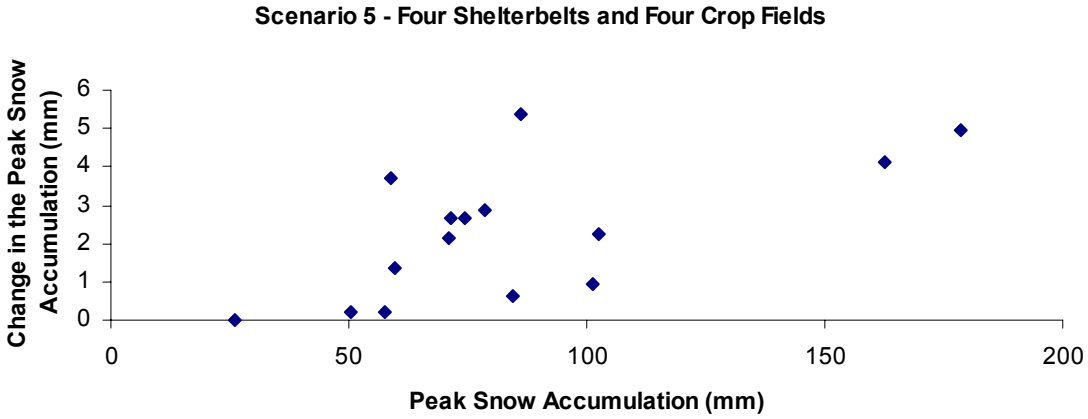

Figure 25. Change in the peak SWE in scenario 5 with respect to scenario 1.

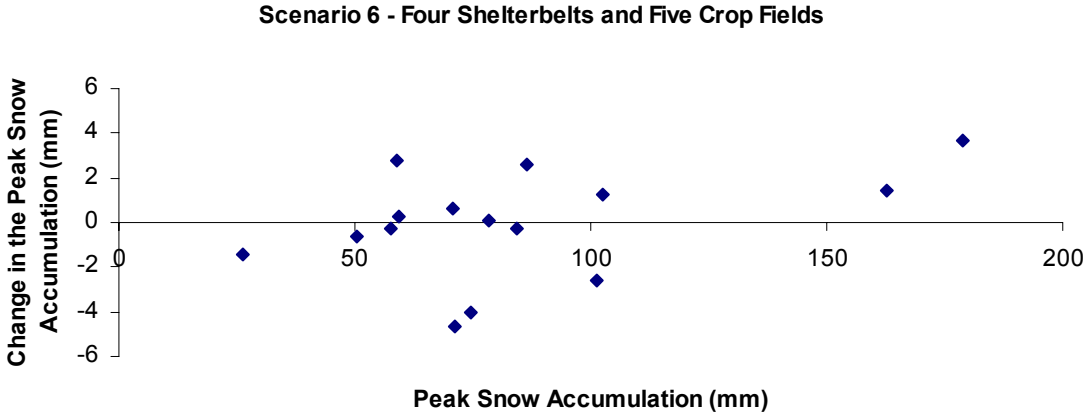

Figure 26. Change in the peak SWE in scenario 6 with respect to scenario 1.

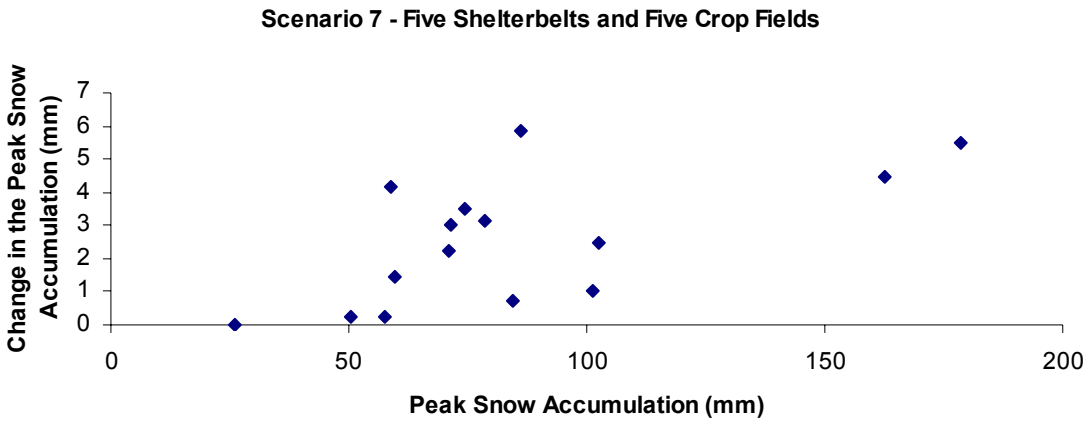

Figure 27. Change in the peak SWE in scenario 7 with respect to scenario 1.

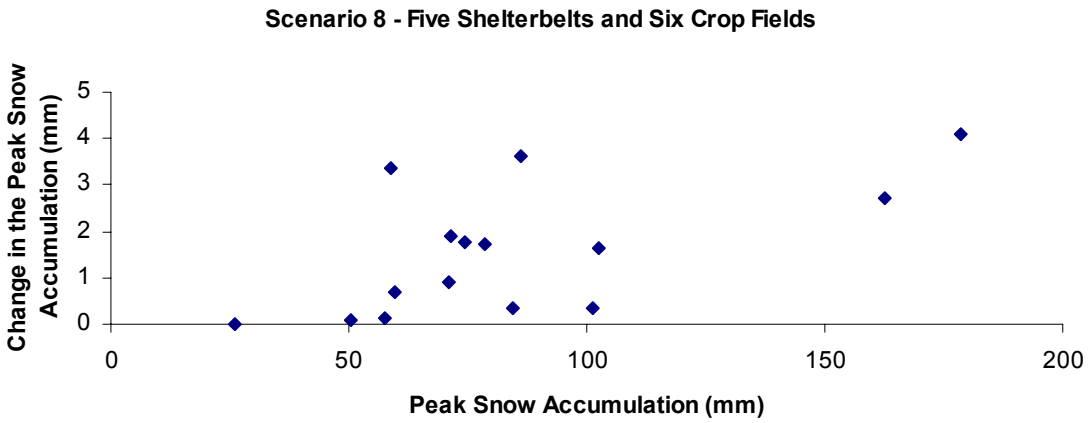

Figure 28. Change in the peak SWE in scenario 8 with respect to scenario 1.

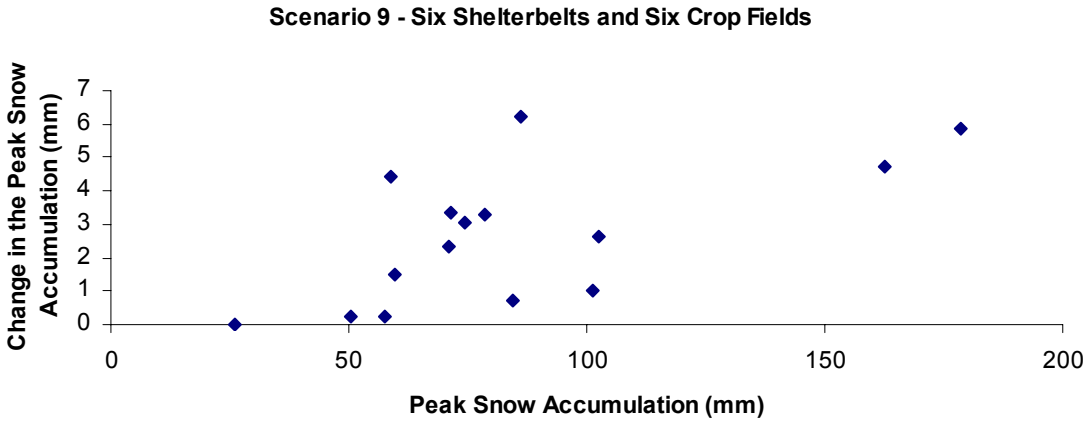

Figure 29. Change in the peak SWE in scenario 9 with respect to scenario 1.

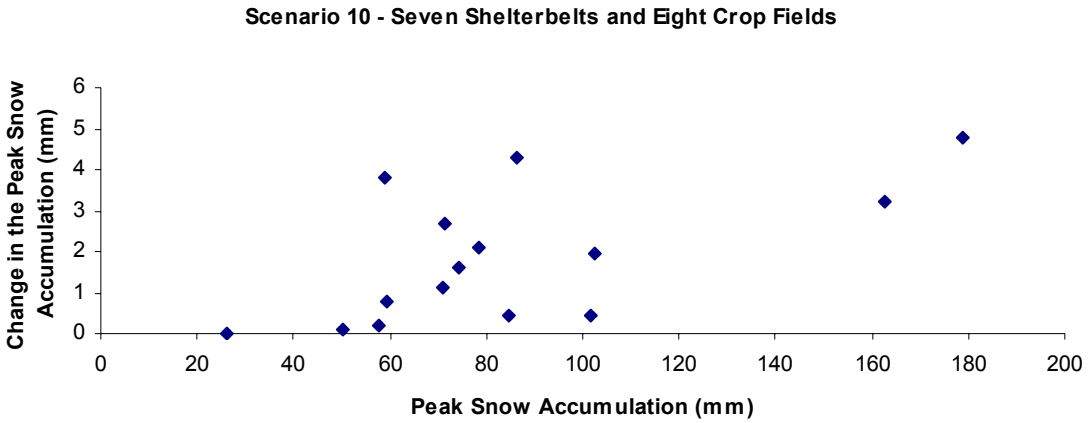

Figure 30. Change in the peak SWE in scenario 10 with respect to scenario 1.

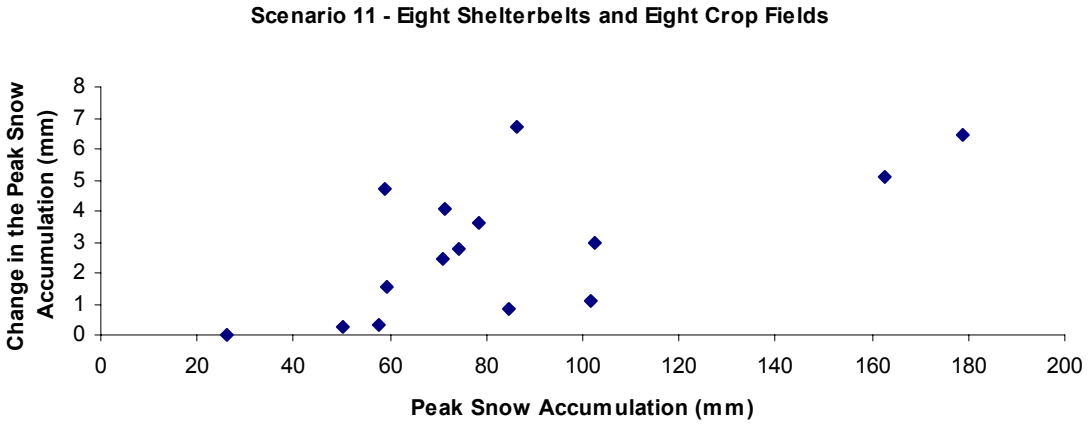

Figure 31. Change in the peak SWE in scenario 11 with respect to scenario 1.

In addition, time-series evaluation of the simulated snow accumulation for the crop field HRUs and shelterbelt HRUs is demonstrated in Figure 32 for a typical dry season (1999-2000), Figure 33 for a typical medium season (2004-2005), and Figure 34 for a typical snowy season (2005-2006). The gauge wind undercatch corrected seasonal snowfall is shown, being 104 mm, 145 mm, and 199 mm for 1999-2000, 2004-2005, and 2005-2006, respectively. Figure 32 shows that adding three (scenario 4), and five shelterbelts (scenario 7) has a minimal effect on snow accumulation over the half section of land under the dry condition, and the peak SWE for shelterbelts is no greater than the cumulative snowfall indicating little wind redistribution of snow in a dry year. Under medium and wet conditions, both scenario 4 and scenario 7 for the shelterbelt show an increase in peak SWE above the cumulative snowfall (Figures 33 and 34). This is attributed to substantial blowing snow transport from the crop fields to the shelterbelts under medium and wet conditions, whereas the blowing snow transport is severely

suppressed under the dry condition. This is also evident in Figures 35 to 44 that show the difference between peak SWE on crop field and shelterbelt. Figures 35 to 44 all demonstrate that as a result of blowing snow transport, higher peak SWE is found in shelterbelts than in crop fields, except for the driest conditions (i.e. snowfall = 55 mm or less).

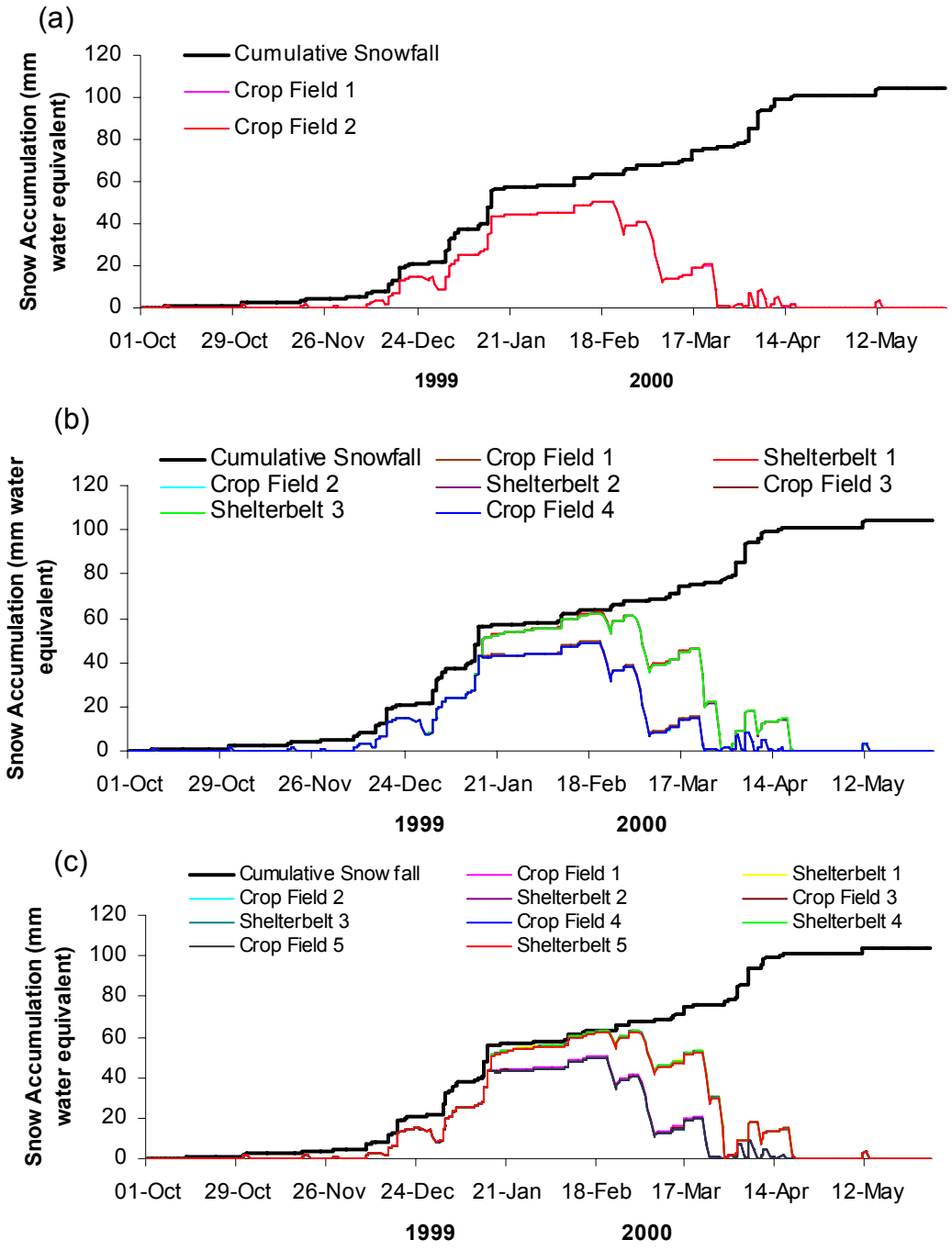

Figure 32. Simulated snow accumulation evolution on crop fields and shelterbelts HRUs during dry season (1999-2000). (a) Scenario 1, (b) scenario 4, and (c) scenario 7.

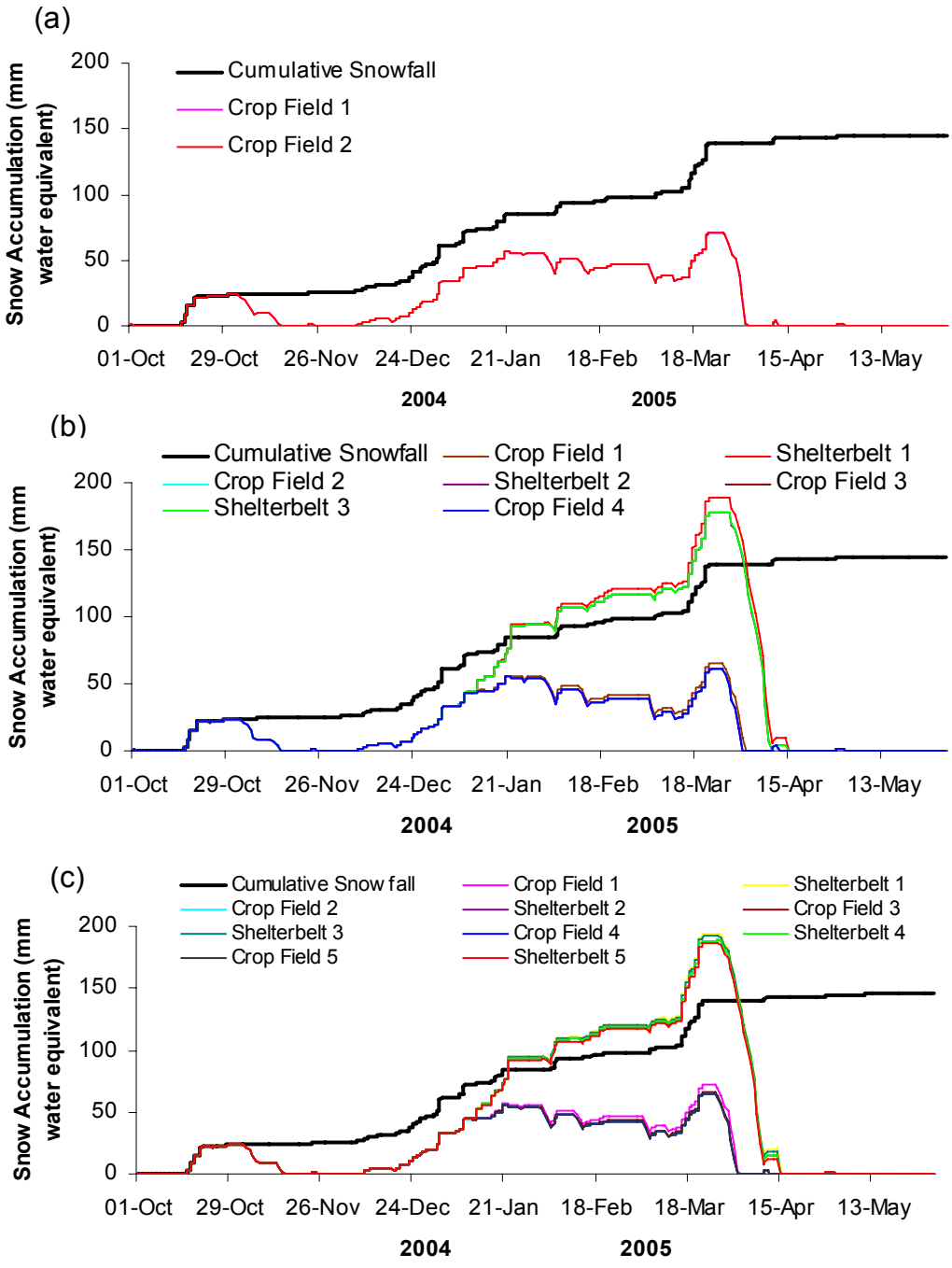

Figure 33. Simulated snow accumulation evolution on crop fields and shelterbelts HRUs during medium season (2004-2005). (a) Scenario 1, (b) scenario 4, and (c) scenario 7.

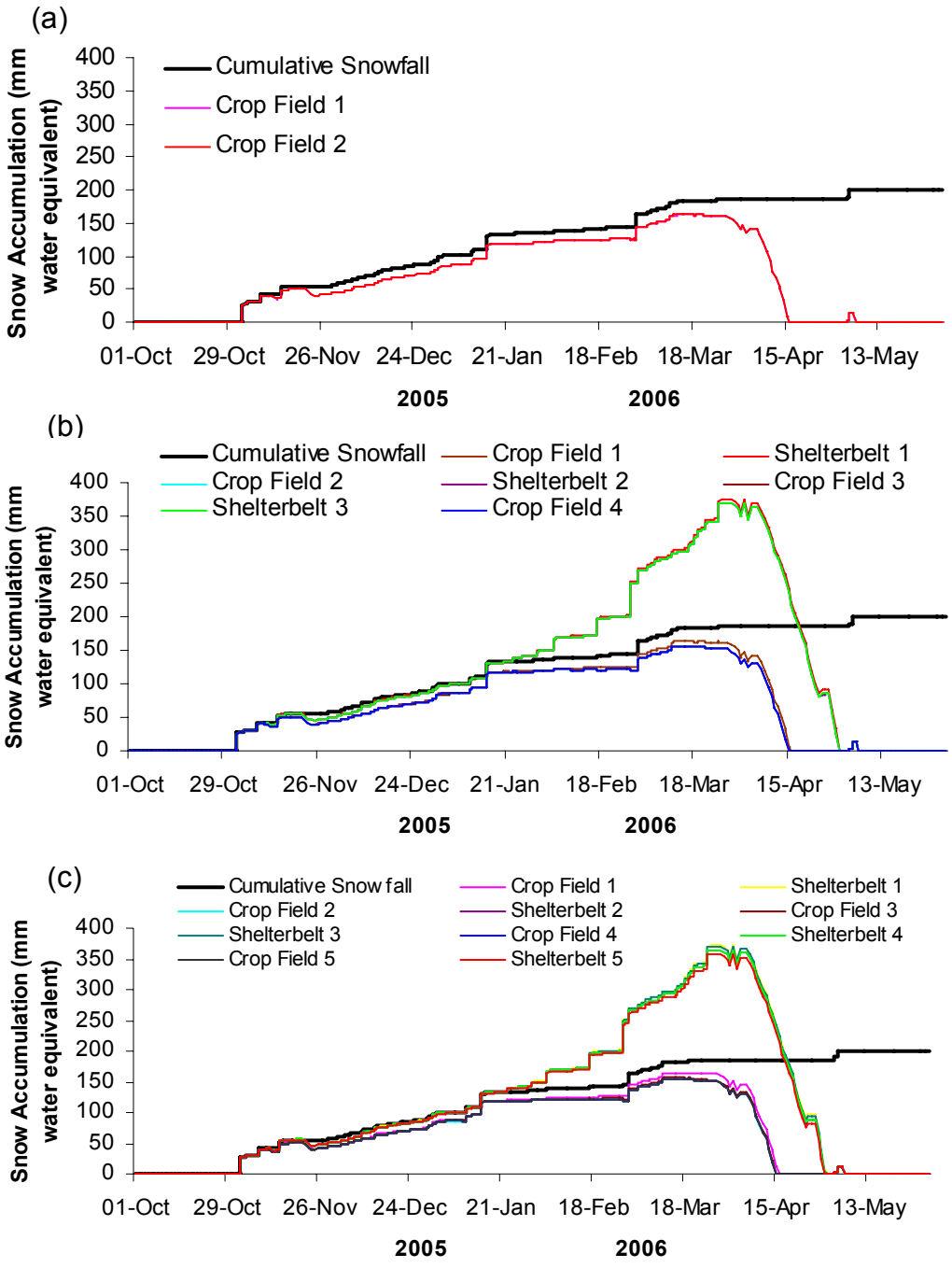

Figure 34. Simulated snow accumulation evolution on crop fields and shelterbelts HRUs during wet season (2005-2006). (a) Scenario 1, (b) scenario 4, and (c) scenario 7.

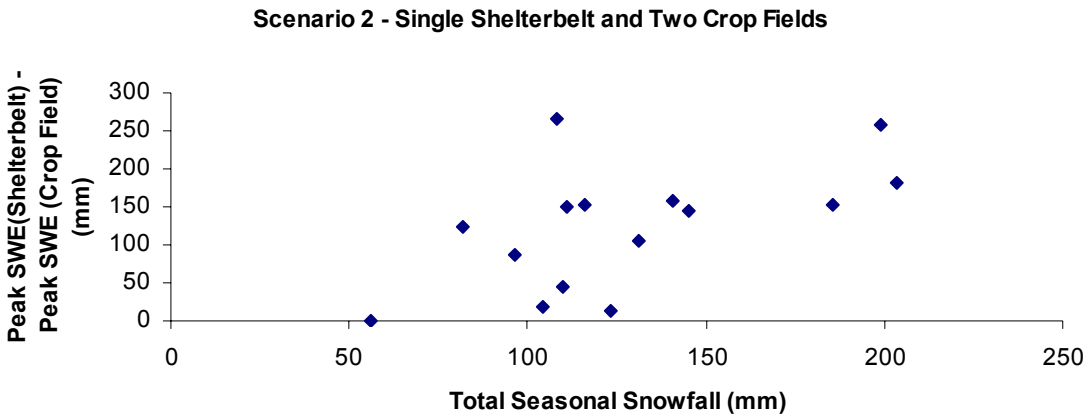

Figure 35. Difference of the peak SWE on shelterbelt and on crop field for scenario 2.

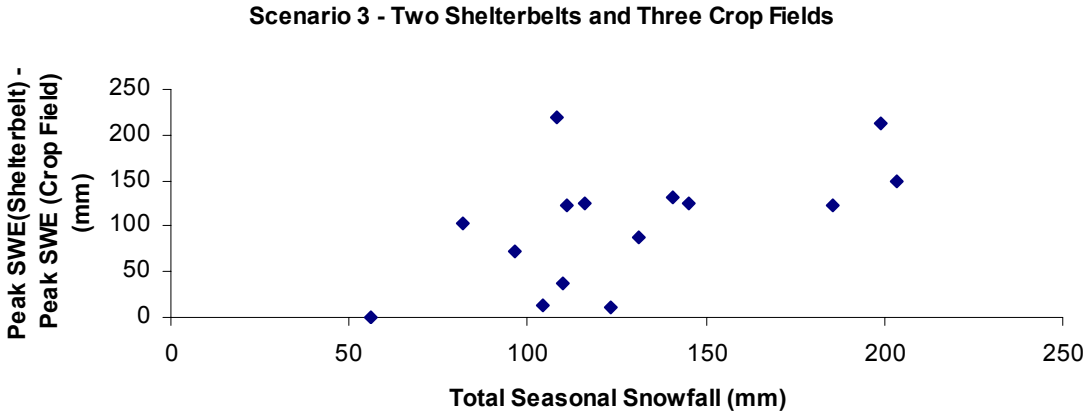

Figure 36. Difference of the peak SWE on shelterbelt and on crop field for scenario 3.

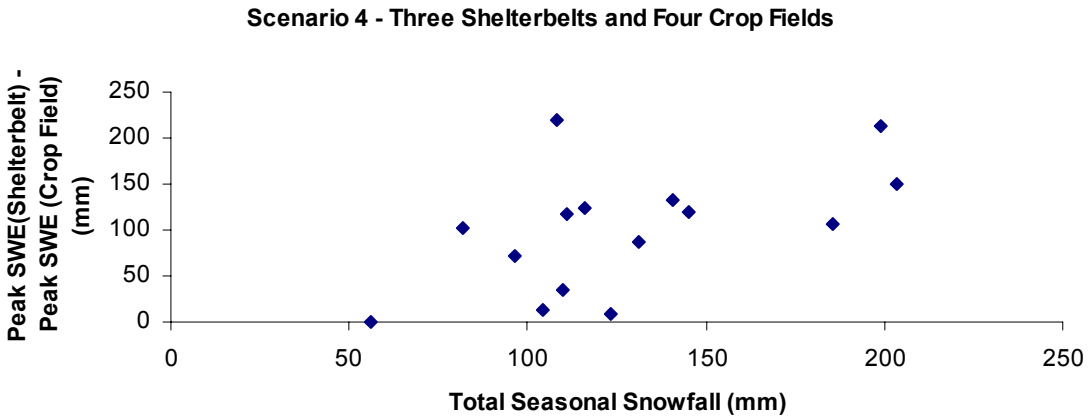

Figure 37. Difference of the peak SWE on shelterbelt and on crop field for scenario 4.

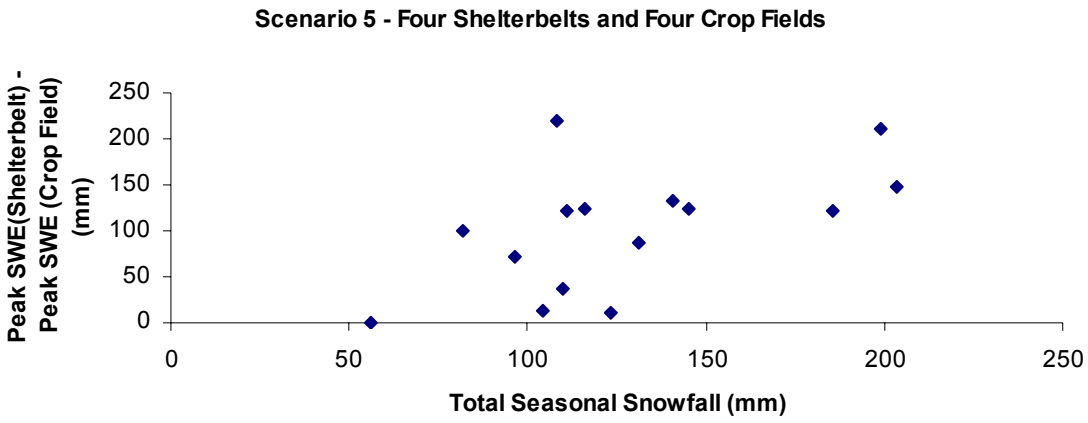

Figure 38. Difference of the peak SWE on shelterbelt and on crop field for scenario 5.

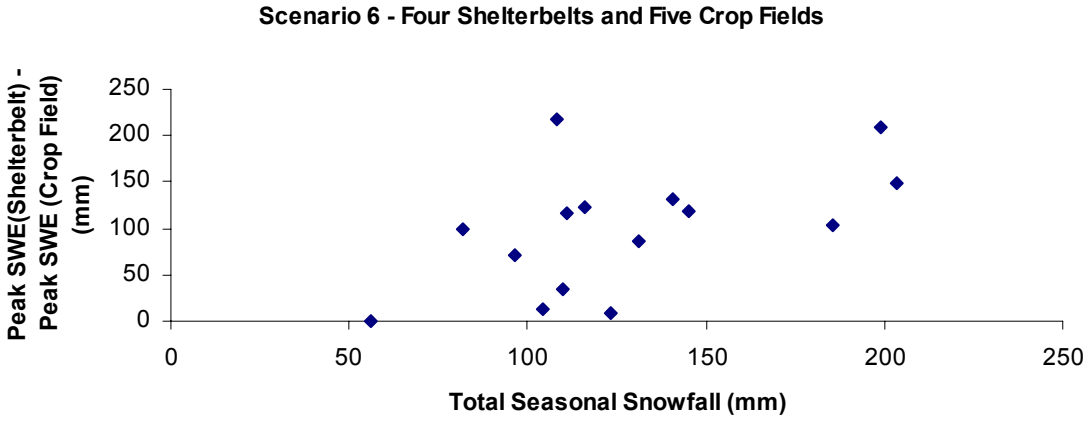

Figure 39. Difference of the peak SWE on shelterbelt and on crop field for scenario 6.

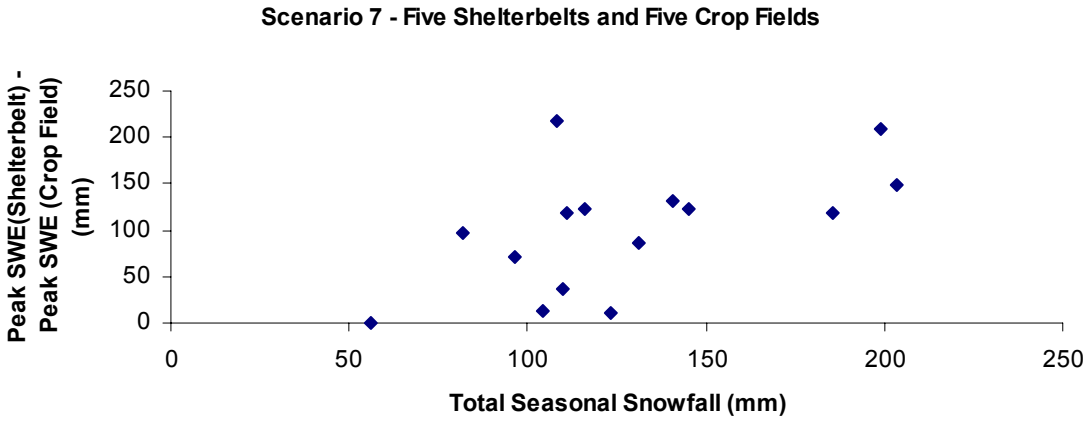

Figure 40. Difference of the peak SWE on shelterbelt and on crop field for scenario 7.

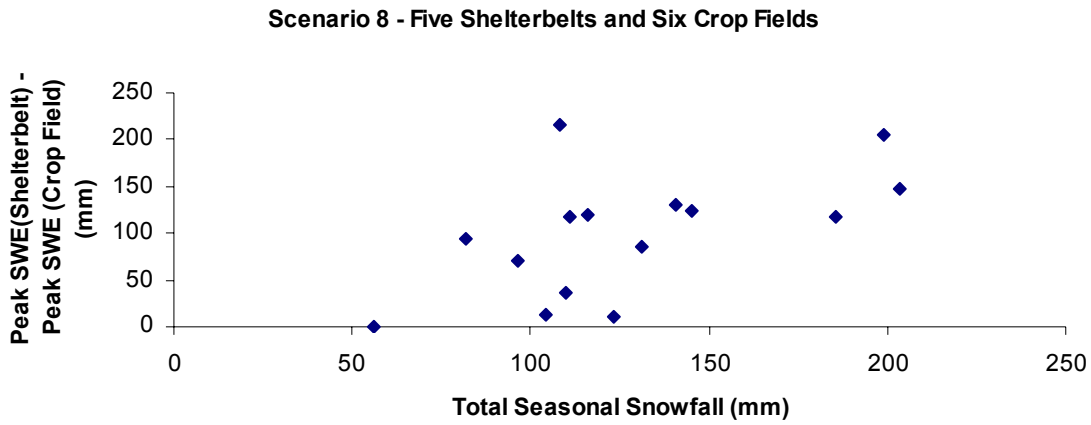

Figure 41. Difference of the peak SWE on shelterbelt and on crop field for scenario 8.

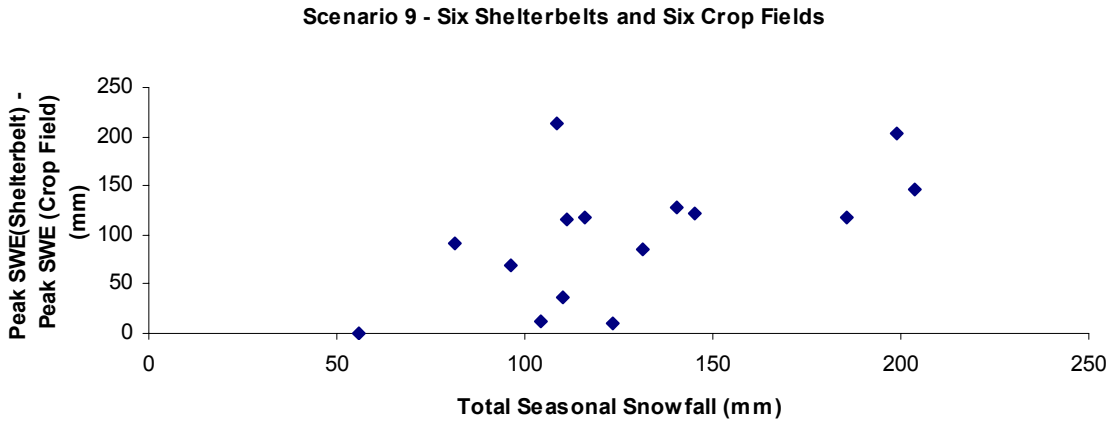

Figure 42. Difference of the peak SWE on shelterbelt and on crop field for scenario 9.

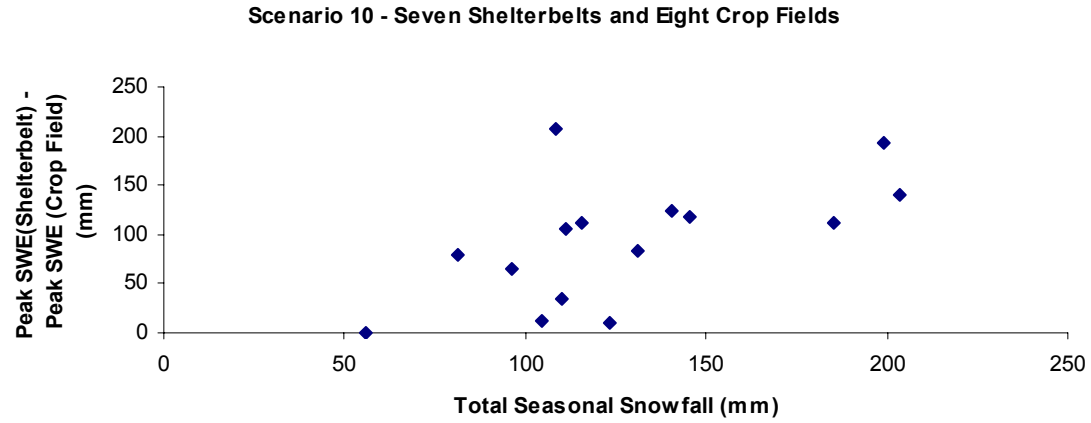

Figure 43. Difference of the peak SWE on shelterbelt and on crop field for scenario 10.

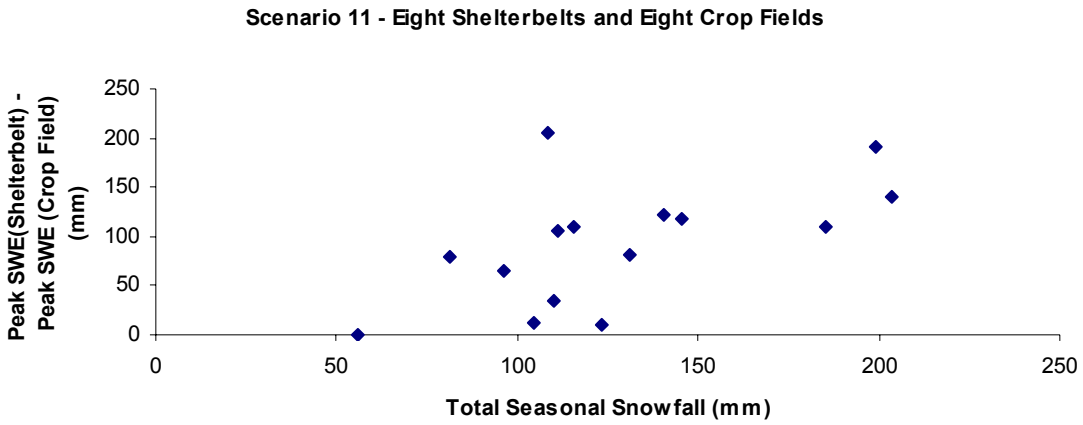

Figure 44. Difference of the peak SWE on shelterbelt and on crop field for scenario 11.

5.2.2 Blowing Snow Sublimation Loss

The seasonal blowing snow sublimation loss (subl) from crop field and shelterbelt HRUs was estimated for the 15-year period, and the area-weighted average sublimation was calculated over the entire half section land using Equation 8. The area-weighted average sublimation is the blowing snow sublimation loss from the entire half section of land,

$$subl(half\_\sec) = \frac{\sum_{i=1}^{n1} subl(crop\_field_i) \times Area(crop\_field_i) + \sum_{j=1}^{n2} subl(shelterbelt_j) \times Area(shelterbelt_j)}{Area(crop\_field) + Area(shelterbelt)} \quad [8]$$

where $subl(crop\_field_i)$ and $subl\ (shelterbelt_j)$ are the simulated sublimation from crop field (i) and shelterbelt (j), and $Area(crop\_field_i)$ and $Area\ (shelterbelt_j)$ are the area at crop field (i) and shelterbelt (j), with i and j being the number of crop field and shelterbelt in each scenario. $n1$ and $n2$ are the total number of crop fields and shelterbelts, respectively. $Area(crop\_field)$ and $Area\ (shelterbelt)$ are the respective total area of crop field and shelterbelt in each scenario.

The cumulative seasonal sublimation was calculated for the entire half section of land during the 15-year period and is shown in Figure 45. A steady decline in the blowing snow sublimation loss is found as the scenario proceeds from 1 (no shelterbelt) to 11. The decline also varies with the climate condition, with little or no decline in dry seasons (e.g. 1999-2000, 2000-2001) and a large decline in wet seasons (e.g. 2005-2006). In addition, the 15-year (1996-2011) averaged seasonal sublimation was estimated for the entire half section of land for each of the 11 scenarios and is shown in Figure 46. The 15-year averaged seasonal sublimation from the half section of land in scenarios 2 to 11 (i.e. half section land with various number of shelterbelts) was also compared to that in the scenario 1 (i.e. half section land with no shelterbelt), and this is shown in Figure 47 as the "change in seasonal sublimation". The figure demonstrates that increasing shelterbelts on the half section of land leads to reducing the blowing snow sublimation loss, from

15% in scenario 2 to ~50% in scenario 11, corresponding to ~1.3 mm and 4 mm less sublimation loss, respectively.

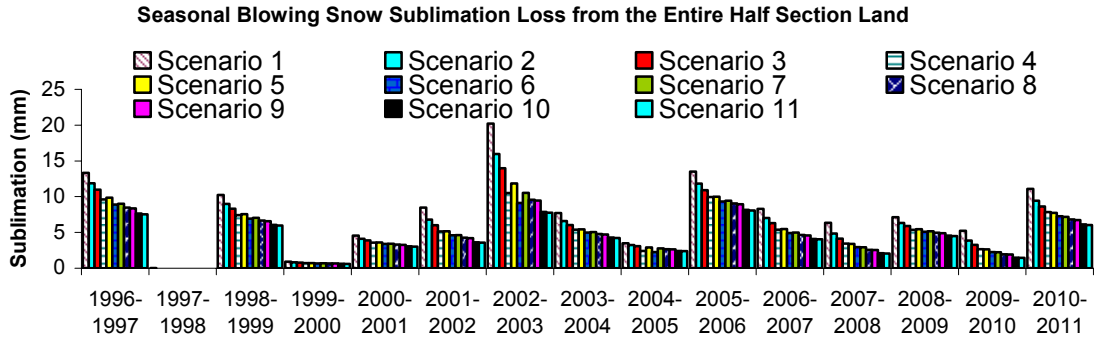

Figure 45. The simulated cumulative seasonal blowing snow sublimation loss from the entire half section land during 15-year period (1 October 1996-14 April 2011) for the 11 shelterbelt scenarios.

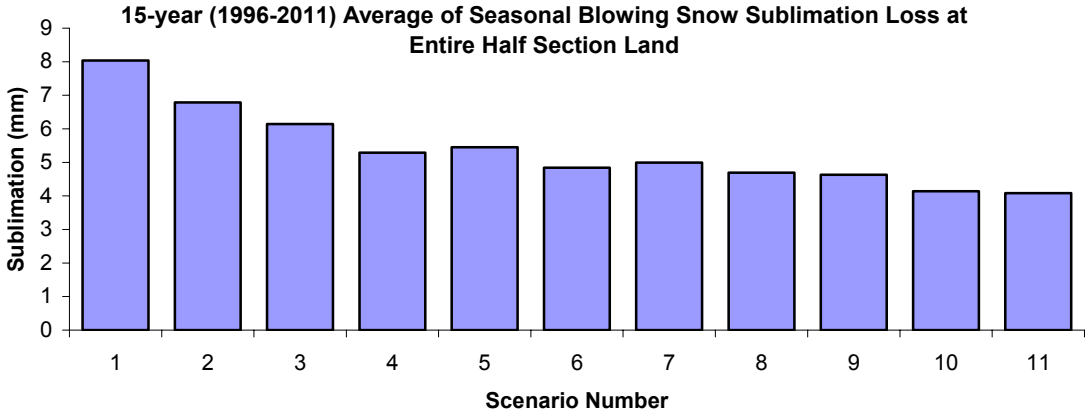

Figure 46. The 15-year (1996-2011) average of cumulative seasonal blowing snow sublimation loss from the half section land for the 11 scenarios.

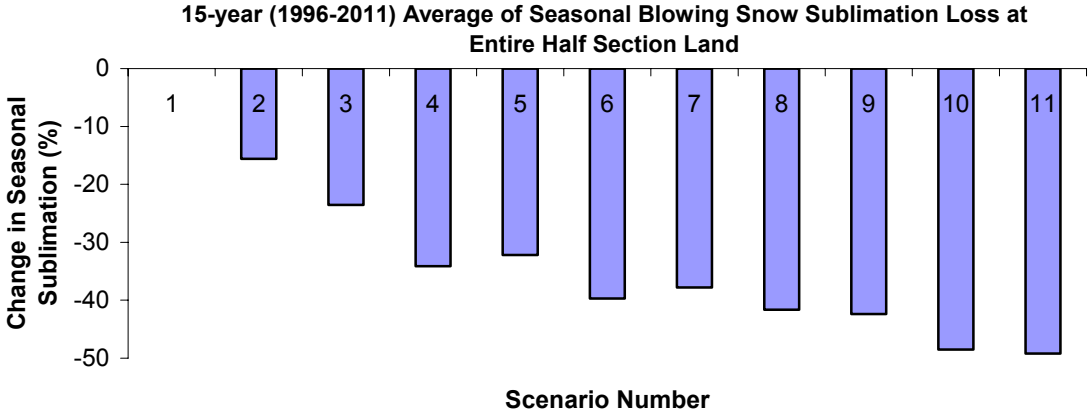

Figure 47. Change in the 15-year (1996-2011) average seasonal blowing snow sublimation loss from the half section land. The change is the difference between the average seasonal blowing snow sublimation in scenario 1 and other scenarios.

5.2.3 Blowing Snow Basin Gain and Loss

The shelterbelt model also simulated the blowing snow "basin" gain and loss; the "basin" gain is the blowing snow transport into the half section of land from outside fields, while the basin loss is the snow transport blown out of the half section of land. The cumulative seasonal blowing snow basin gains and losses as well as the net gains (i.e. gain – loss) were calculated for the entire half section of land during the 15-year period. In general shelterbelts had only a small effect on blowing snow gains to the half section. Blowing snow losses were completely prevented by the presence of shelterbelts. Without shelterbelts losses were minimal in dry years and up to 2.3 mm SWE in the snowiest years.

6. Conclusions

A “shelterbelt blowing snow model” was successfully developed in the Cold Regions Hydrological Model platform (CRHM) for the narrowly and widely spaced shelterbelt sites located near Conquest, Saskatchewan. 15-years (1996-2011) of meteorological data were gathered and cleaned from the Outlook PFRA station and were used to drive the shelterbelt model. A comparison between the modelled and measured snow accumulation for one day in February 2011 on the narrowly and widely spaced shelterbelt sites demonstrated an acceptable predictive performance for the model. In light of that, the shelterbelt model was used for developing shelterbelt scenarios on a virtual half section of land covered with grain stubble. Eleven shelterbelt scenarios with various configurations for the crop fields and shelterbelts were created, including no shelterbelt, a single shelterbelt, and several shelterbelts with narrow to wide spacings. The seasonal peak snow accumulation on the crop field, shelterbelt, and the entire half section of land was estimated along with blowing snow sublimation loss from the half section, and snow transport gain and loss from outside of the half section. These results indicate that there is increasing peak seasonal snow accumulation and declining seasonal blowing snow sublimation loss with an increasing the number of shelterbelts. Shelterbelts also reduced blowing snow transport losses from the half section. These effects are most prominent for snowier winter seasons compared to dry seasons when shelterbelts had little effect on snow accumulation, sublimation or transport.

Reference

Annandale, J.G., Jovanovic, N.Z., Benadé, N. and Allen, R.G. 2002. Software for missing data error analysis of Penman-Monteith reference evapotranspiration. *Irrigation Science* **21**: 57-67.

Dyunin, A. K. 1959. Fundamentals of the theory of snow drifting. *Izv. Sibirsk. Otdel. Akad. Nauk USSR*, *12*, 11-24. (Translated to English by G. Belkov, Tech. Trans. 952, Na. Res. Counc. of Can., Ottawa, 1961).

Essery, R., Li, L. and Pomeroy, J. 1999. A distributed model of blowing snow over complex terrain. *Hydrological Processes* **13**: 2423-2438.

Fang, X. and Pomeroy, J.W. 2007. Snowmelt runoff sensitivity analysis to drought on the Canadian Prairies. *Hydrological Processes* **21**: 2594-2609.

Fang, X. and Pomeroy, J.W. 2009. Modelling blowing snow redistribution to prairie wetlands. *Hydrological Processes* **23**: 2557-2569.

Fang, X., Pomeroy, J.W., Westbrook, C.J., Guo, X. Minke, A.G. and Brown, T. 2010. Prediction of snowmelt derived streamflow in a wetland dominated prairie basin. *Hydrology and Earth System Sciences* **14**: 991-1006.

Garnier, B.J. and Ohmura, A. 1970. The evaluation of surface variations in solar radiation income. *Solar Energy* **13**: 21-34.

Gray, D.M. and Landine, P.G. 1987. Albedo model for shallow prairie snow covers. *Canadian Journal of Earth Sciences* **24**: 1760-1768.

Gray, D.M. and Landine, P.G. 1988. An energy-budget snowmelt model for the Canadian Prairies. *Canadian Journal of Earth Sciences* **25**: 1292-1303.

Li, L. and Pomeroy, J.W. 1997a. Estimates of threshold wind speeds for snow transport using meteorological data. *Journal of Applied Meteorology* **36**: 205-213.

Li, L. and Pomeroy, J.W. 1997b. Probability of blowing snow occurrence by wind. *Journal of Geophysical Research* **102**: 21,955-21,964.

Liston, G.E. and Sturm, M. 1998. A snow-transport model for complex terrain. *Journal of Glaciology* **44**: 498-516.

MacDonald, M.K., Pomeroy, J.W. and Pietroniro, A. 2009. Parameterizing redistribution and sublimation of blowing snow for hydrological models: tests in a mountainous subarctic catchment. *Hydrological Processes* **23**: 2570-2583.

Pomeroy, J.W. 1989. A process-based model of snow drifting. *Annals of Glaciology* **13**: 237-240.

Pomeroy, J.W., Gray, D.M. and Landine, P.G. 1993. The prairie blowing snow models: characteristics, validation, operation. *Journal of Hydrology* **144**: 165-192.

Pomeroy, J. W., and D. M. Gray 1995. *Snow Accumulation, Relocation and Management*, 144 pp., Na. Hydrol. Res. Inst. *Sci. Rep. 7*, Environment Canada, Saskatoon.

Pomeroy, J.W. and Li, L. 2000. Prairie and Arctic areal snow cover mass balance using a blowing snow model. *Journal of Geophysical Research* **105**: 26619-26634.

Pomeroy, J.W., Gray, D.M., Brown, T., Hedstrom, N.R., Quinton, W., Granger, R.J. and Carey, S. 2007. The Cold Regions Hydrological Model, a platform for basing process representation and model structure on physical evidence. *Hydrological Processes* **21**: 2650-2667.

Schmidt, R.A. 1972. Sublimation of wind-transported snow-a model. *Research Paper RM-90*, U.S. Department of Agriculture Forest Service Rocky Mountain Forest and Range Experiment Station, Fort Collins, Colorado, USA.

Shook, K.R. and Pomeroy, J.W. 2011. Synthesis of incoming shortwave radiation for hydrological simulation. *Hydrology Research*, in press.

Tabler, R.D. 1975. Estimating the transport and evaporation of blowing snow. In *Symposium on Snow Management on the Great Plains Proceedings*, Great Plains Agricultural Council Publication, Lincoln, Nebraska, USA, **73**, pp. 85-104..